Generation of keV harmonics and ultrashort waveforms driven by midinfrared lasers

Carlos Hernández-García

carloshergar@jila.colorado.edu

JILA
CU-Boulder and NIST

VNiVERSiDAD D SALAMANCA
CAMPUS DE EXCELENCIA INTERNACIONAL

KITP, August 13th 2014

MARIE CURIE ACTIONS

SEVENTH FRAMEWORK PROGRAMME

People involved

'Generation of keV harmonics and ultrashort waveforms driven by midinfrared lasers'

Agnieszka A. Jaroń-Becker, and Andreas Becker

Tenio Popmintchev, Margaret M. Murnane, and Henry C. Kapteyn

JILA and Department of Physics, University of Colorado Boulder, USA

Luis Plaja

Grupo de Investigación en Óptica Extrema, Universidad de Salamanca, Spain

J.A. Pérez-Hernández

Centro de Láseres Pulsados, CLPU, Salamanca, Spain

supported by DOE, NSF,
Janus supercomputer (Univ. Colorado)

High-order Harmonic Generation (HHG)

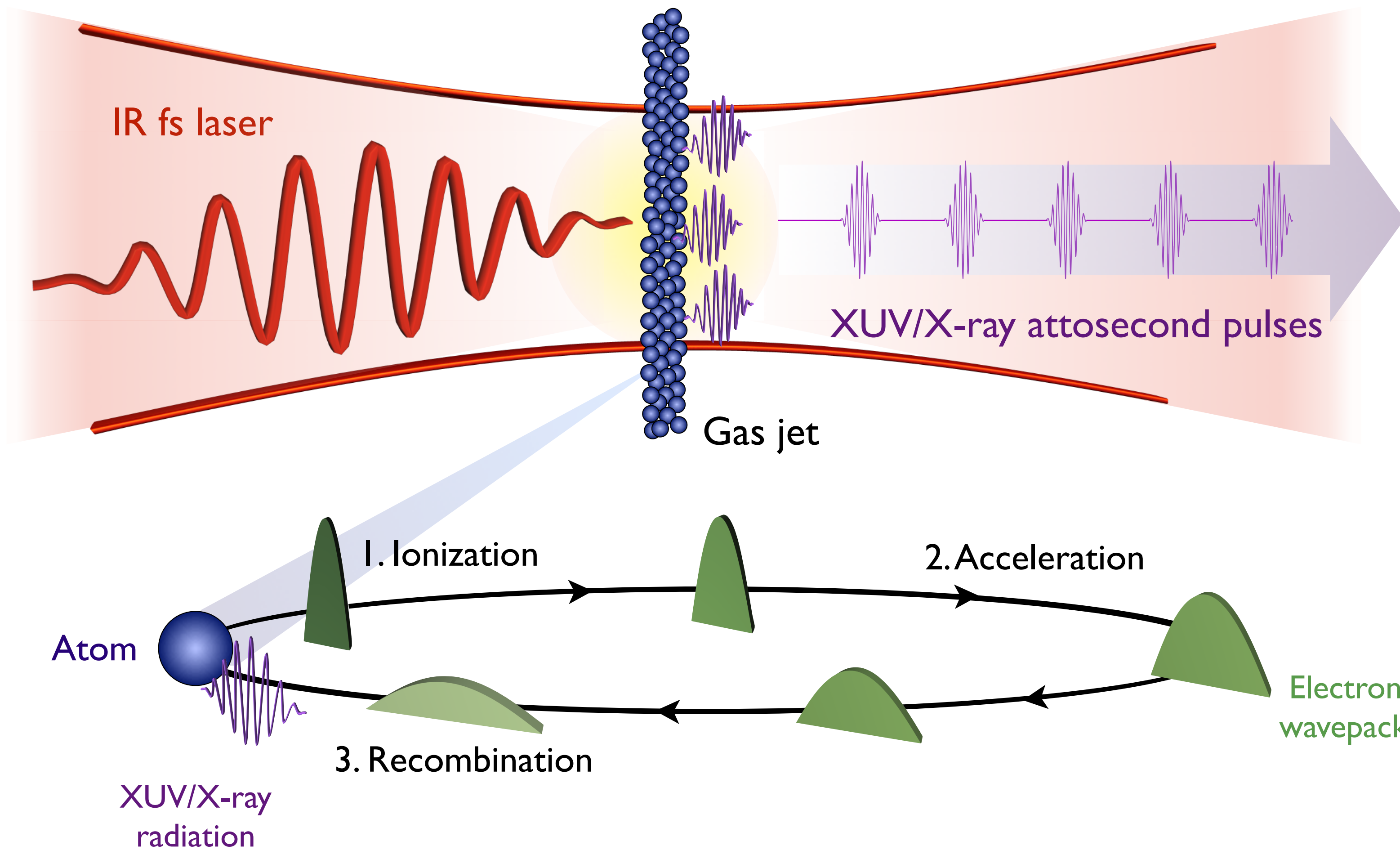

Corkum, PRL 71, 1994 (1993)
Schafer et al. PRL 70 1599 (1993)

High-order Harmonic Generation

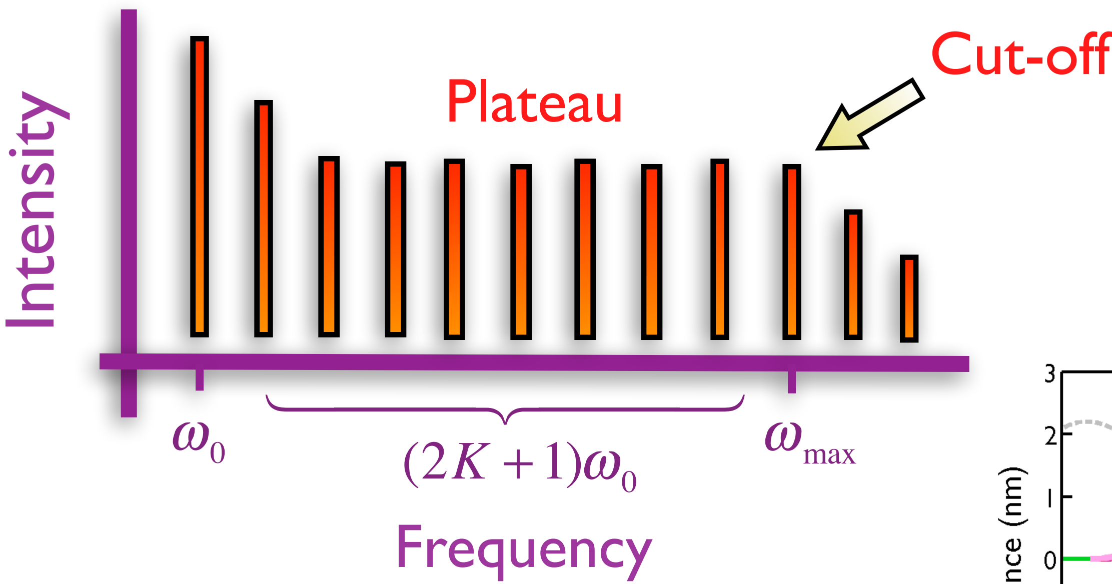

$$\hbar\omega_{\max} \simeq I_p + 3.17U_p \propto I\lambda^2$$

$$U_p = \frac{E_0^2}{4\omega_0^2}$$

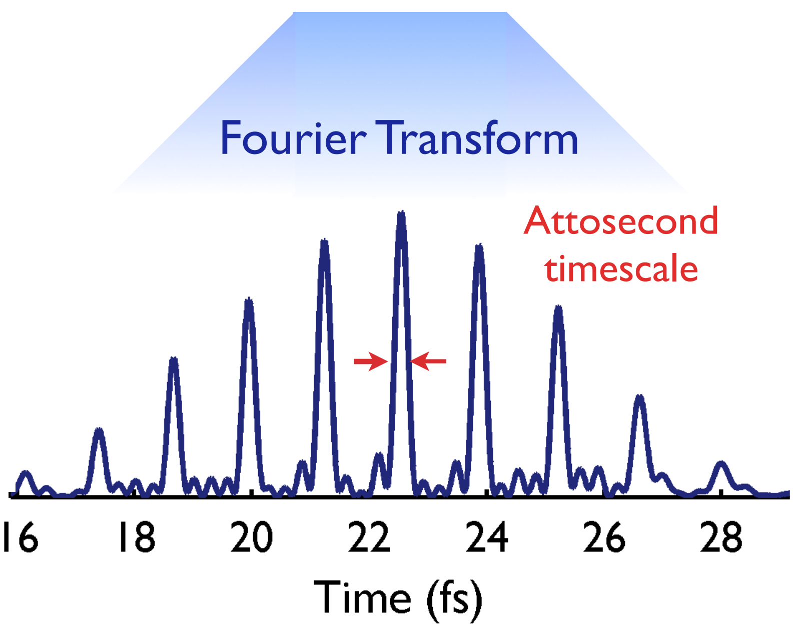

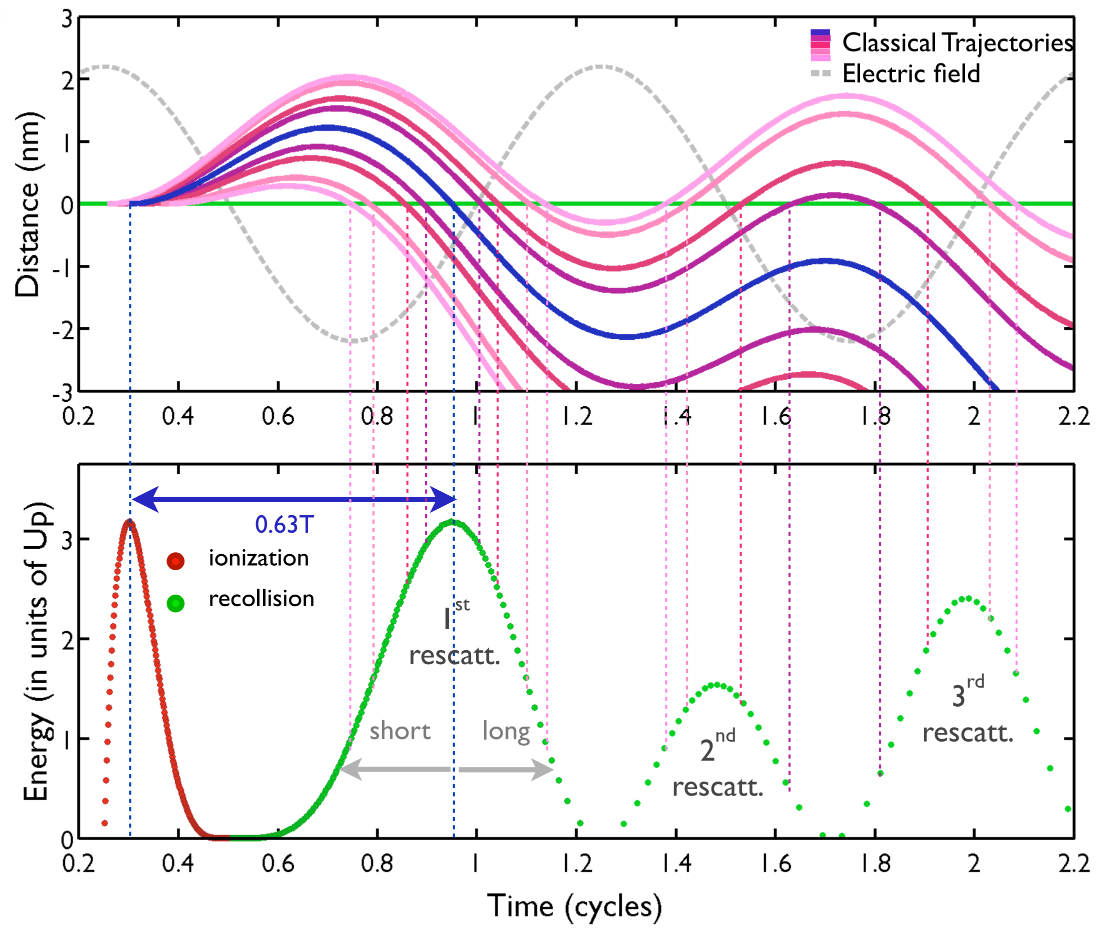

Macroscopic Phase-matching

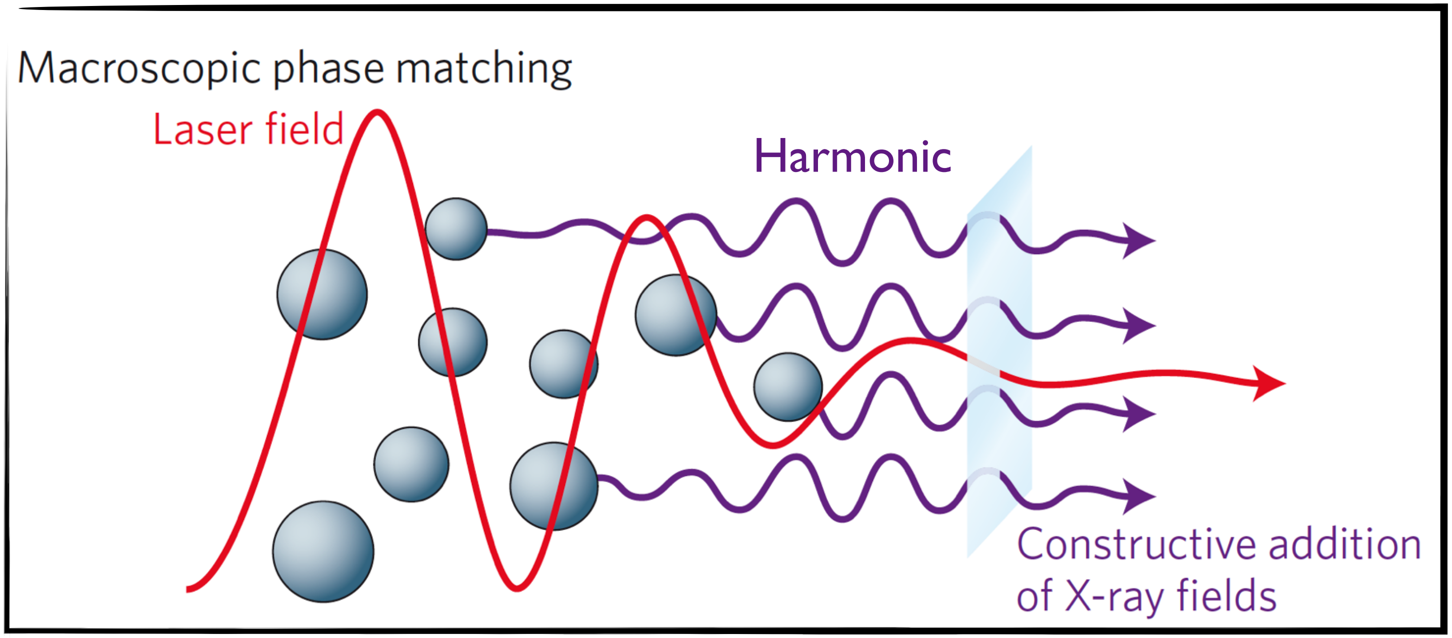

Figure courtesy of T. Popmintchev

Phase mismatch function: $\Delta k_q = k_q - qk_1$

Perfect phase-matching
$\Delta k_q = 0$

P. Saliéres, A. L'Huillier, and M. Lewenstein, PRL, 74, 3776 (1995)
P. Balcou, P. Saliéres, A. L'Huillier, and M. Lewenstein, PRA, 55, 3204 (1996)
A. Rundquist et al, Science 280, 1412 (1998)
M. B. Gaarde, J. L. Tate, and K.J. Schafer J. Phys. B: At. Mol. Opt. Phys. 41 (2008)
T. Popmintchev et al, PNAS 106, 10516 (2009)

The harmonic orchestra

Laser as the orchestra director...

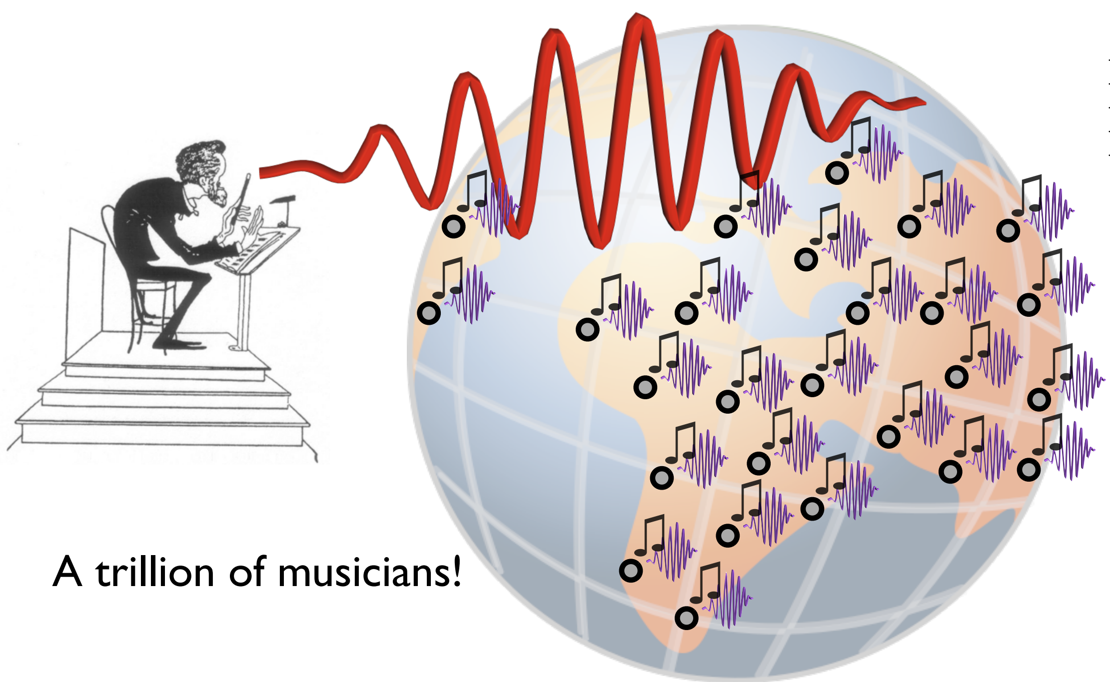

A trillion of musicians!

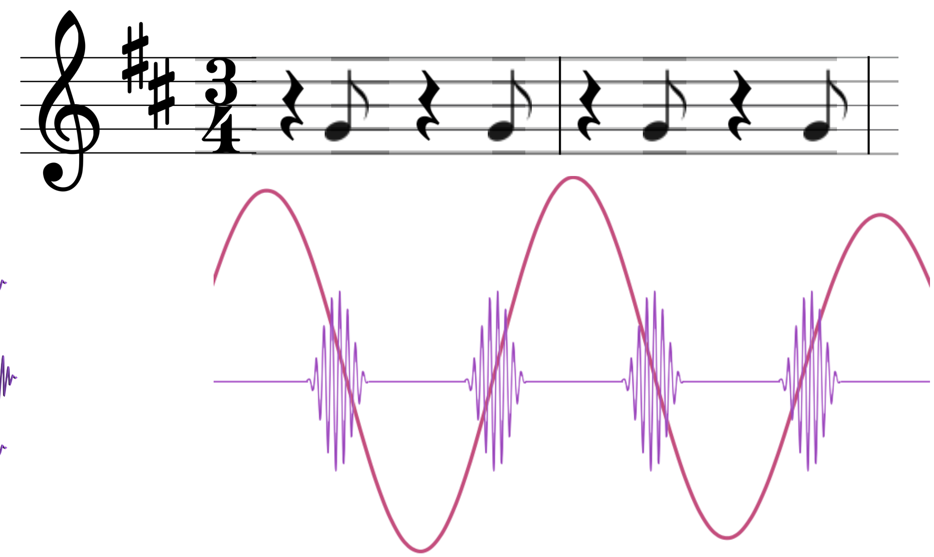

As a result, a *melody* of attosecond pulses
is emitted coherently.

... and each atom of the gas as a musician, emitting
attosecond pulses synchronized with the rhythm
dictated by the laser

Outline

'Generation of keV harmonics and ultrashort waveforms driven by midinfrared lasers'

- Microscopic HHG: single-atom
  - Method: SFA+
  - Multiple rescatterings to produce zeptosecond waveforms
- Macroscopic HHG: phase-matching
  - Method: Discrete Dipole Appoximation
  - Time-gated phase-matching: isolating X-ray attosecond pulses
- Conclusions

Microscopic HHG

Single-atom

Quantum description of HHG

Harmonic emission spectrum is proportional to the power spectrum of dipole acceleration

$$I(\omega) \propto \left|\vec{a}_d(\omega)\right|^2 \qquad \vec{a}_d(\omega) = \int \vec{a}_d(t)\, e^{i\omega t}\, dt$$

$$\vec{a}_d(t) = \frac{1}{m}\left\langle \psi(t)\right|\vec{\nabla}V + \vec{E}\left|\psi(t)\right\rangle$$

$$i\hbar\frac{\partial}{\partial t}\left|\psi(t)\right\rangle = H(t)\left|\psi(t)\right\rangle$$

$$H = \frac{\vec{p}^2}{2m} + V + e\vec{E}\cdot\vec{r}$$

Exact solution: Time Dependent Schrödinger Equation (TDSE) for $\psi(t)$

TDSE is very challenging when:

1. Considering **phase-matching** (involves lot of single-atom calculations)
2. **Long wavelengths** (huge spatio-temporal grid)

We have to use approximations:

✓ The standard way: **SFA** and saddle point M. Lewenstein et al. PRA 49, 2117(1994)

✓ Our choice: **SFA+** J.A. Pérez-Hernández, et al, Opt. Express 17, 9891 (2009)

Strategies for computing HHG

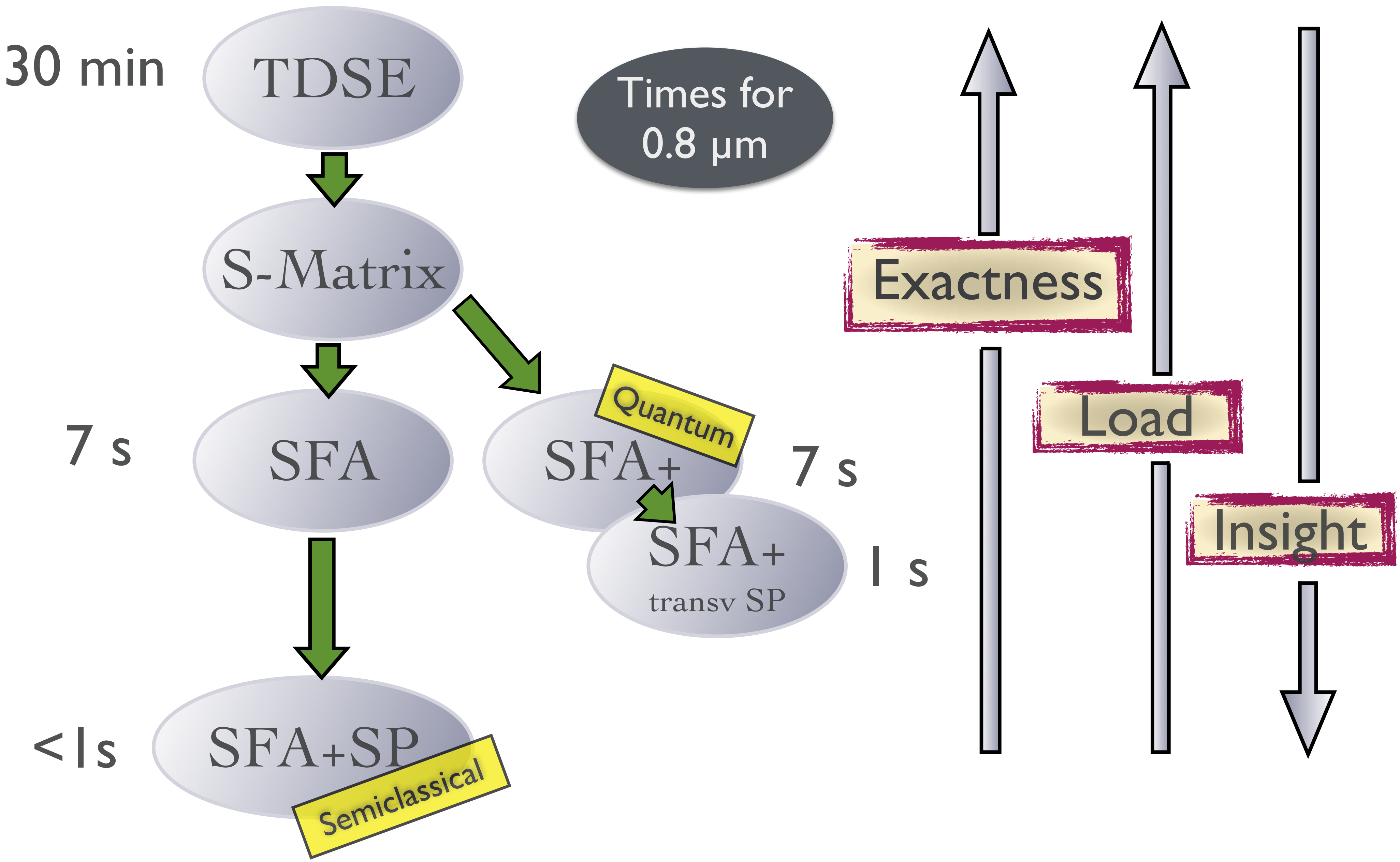

Strategies for computing HHG

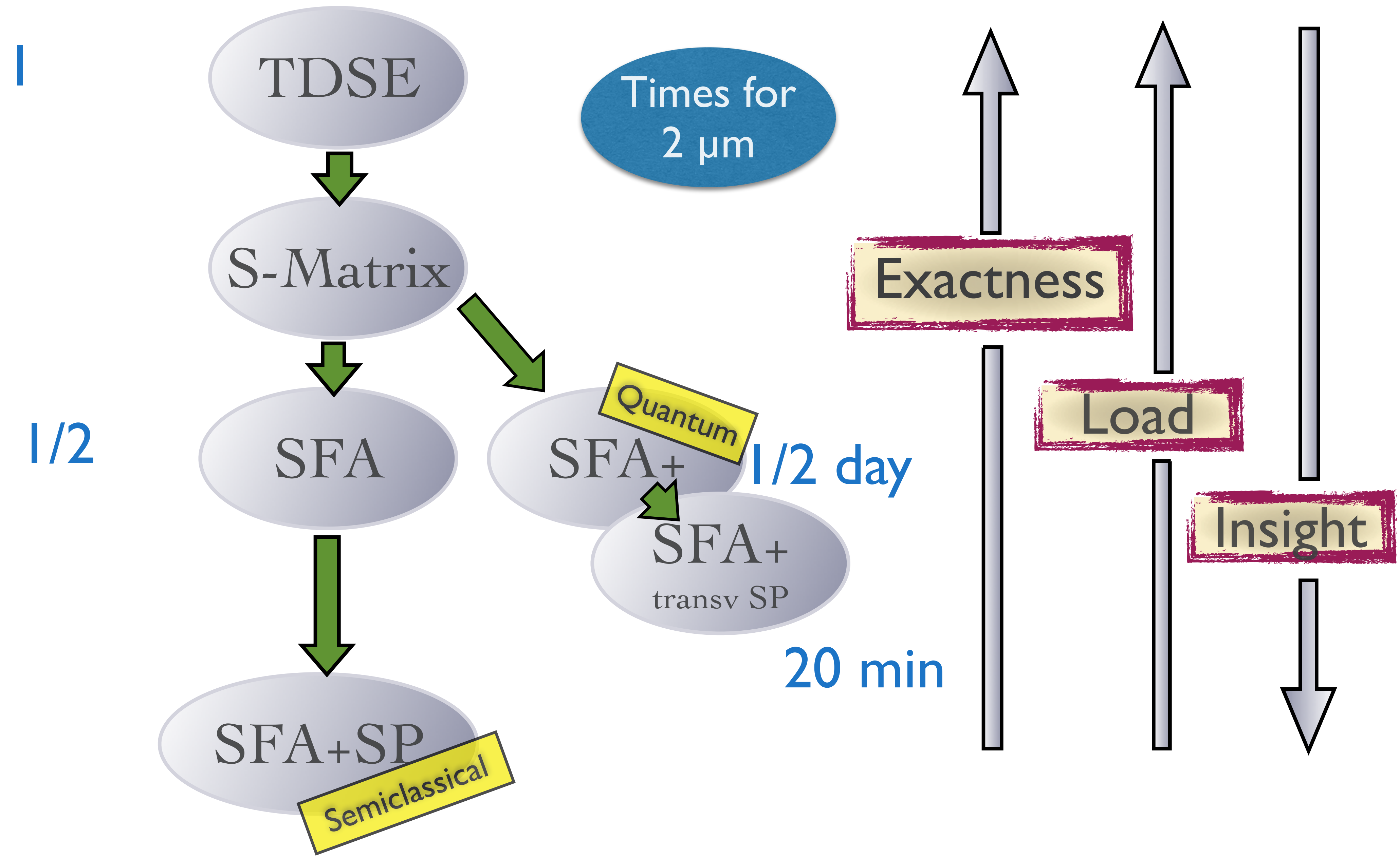

Strategies for computing HHG

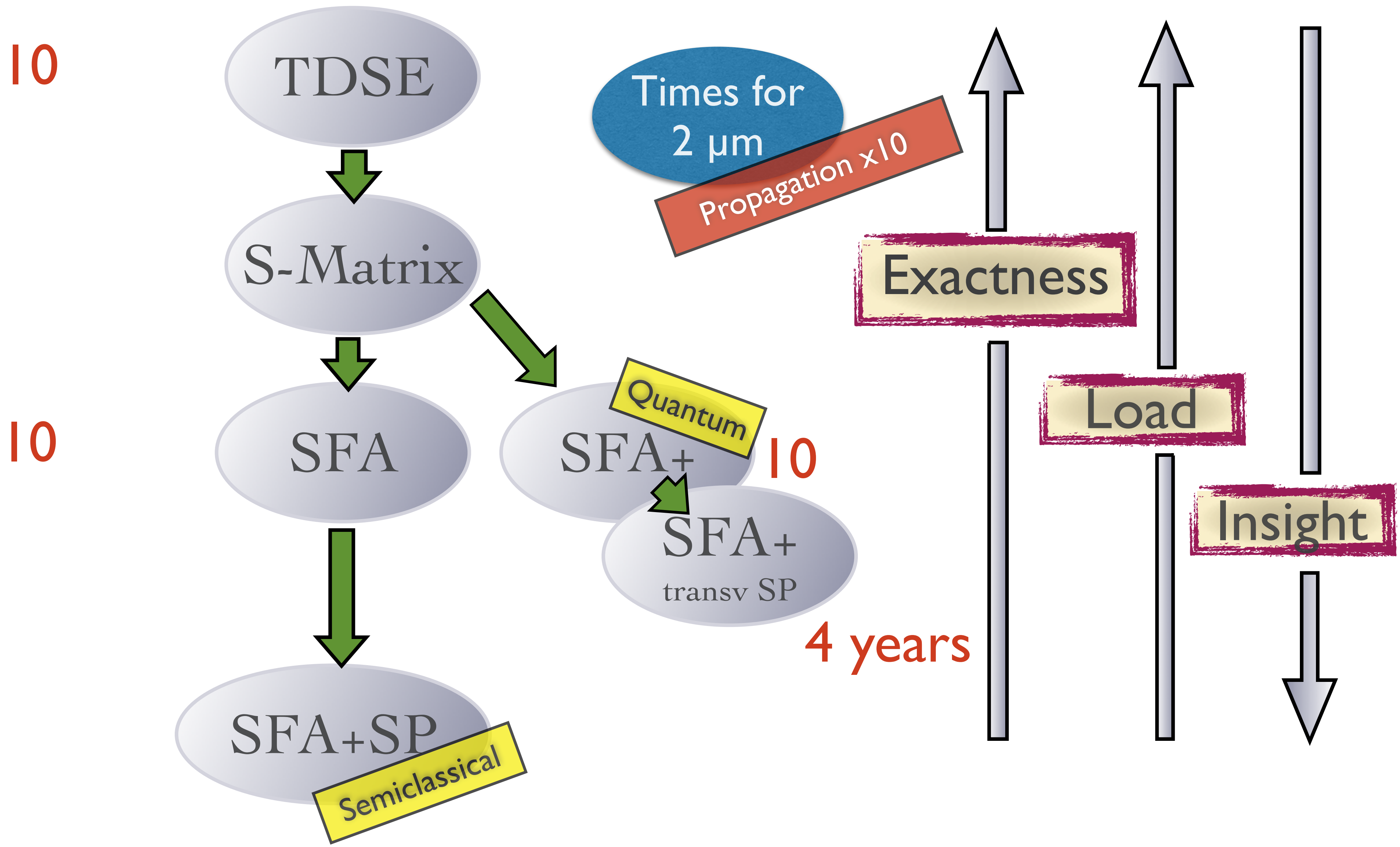

Strategies for computing HHG

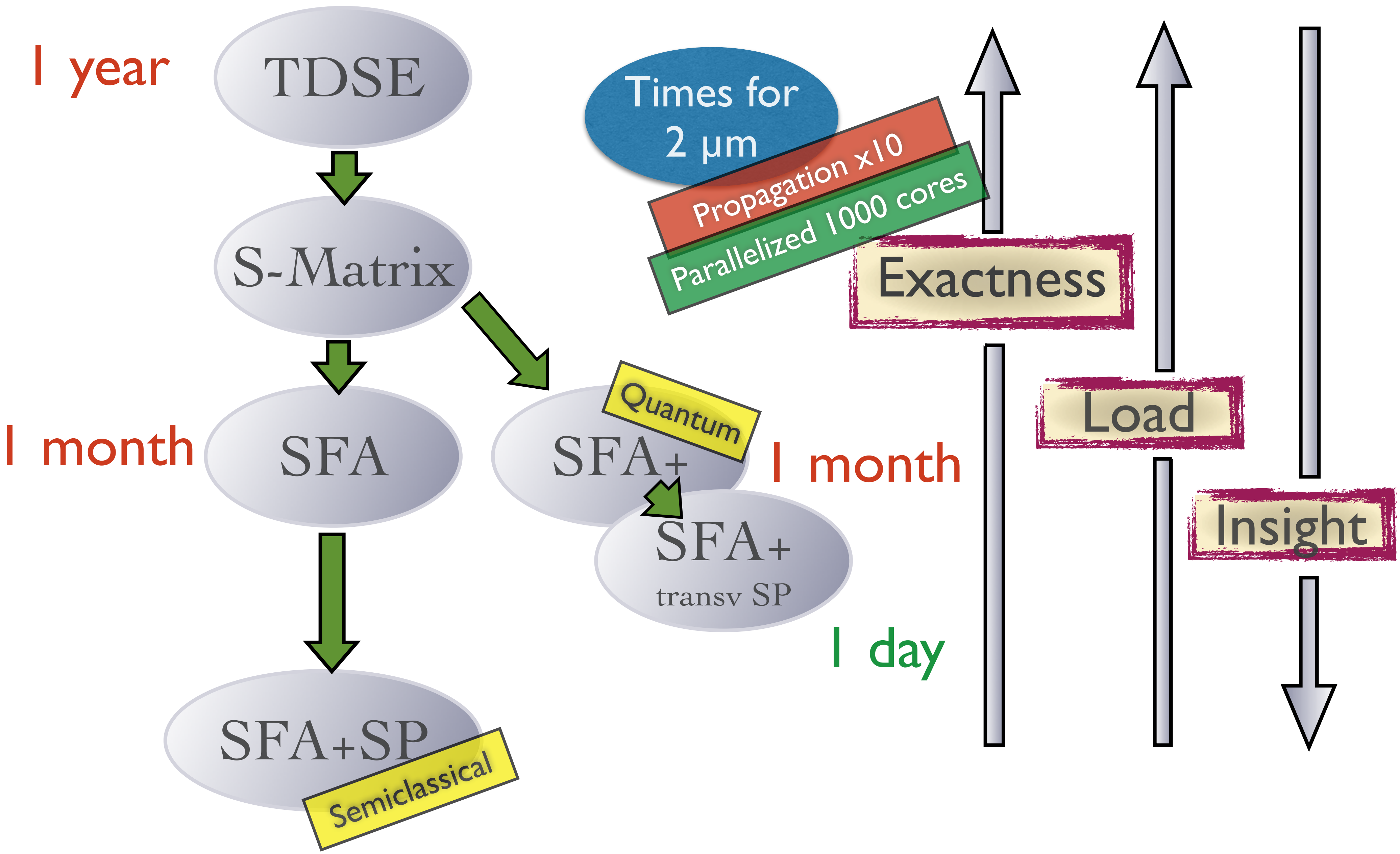

Principles of SFA+

Strong Field Approximation (SFA)

1. Considering the electrons promoted to the continuum to have no possibility to recombine.
2. Neglecting the the bound-state excitations (field-dressing).
3. Considering the electrons as free particles in the continuum.

$$a(\mathbf{k},t) = -\frac{i}{\hbar} C_F \int_{t_0}^{t} dt_1 \langle \phi_0 | \hat{a} | \mathbf{k} \rangle e^{-i\frac{1}{\hbar} S(\mathbf{k},t,t_1)} V_i(\mathbf{k},t_1) \langle \mathbf{k} | r^{-n} | \phi_0 \rangle$$

Transition back to ground state

Transition into the continuum at time t_1

Evolution as a free electron

$$S(\mathbf{k},t,t_1) = \int_{t_1}^{t} [\epsilon(\mathbf{k},\tau) - \epsilon_0]\, d\tau$$

$$V_i(t) = -(q/mc)A(t)p_z + q^2/(2mc^2)A^2(t)$$

$$\epsilon(\mathbf{k},\tau) = \hbar^2 k^2/2m - (\hbar q/mc)A(\tau)k_z + q^2 A^2(\tau)/(2mc^2)$$

Extended Field Approximation (SFA+)

To include the possibility of atomic bound-state excitations (field-dressing).

$$a(t) = a_b(t) + a_d(t) + c.c.$$

$$a_d(\mathbf{k},t) \simeq -\left[1 + \frac{k^2/2m - \epsilon_0}{\Delta_s}\right] a_b(\mathbf{k},t)$$

$$\Delta_s = \langle V_i(t) \rangle = (1/\delta t_s) \int_{t-\delta t_s}^{t} \left[-(q\hbar/mc)A(\tau)k_z + (q^2/2mc^2)A^2(\tau)\right] d\tau$$

J.A. Pérez-Hernández, L. Roso and L. Plaja, Opt. Express 17, 9891 (2009)

J.A. Pérez-Hernández, C. Hernández-García, J. Ramos, E. Conejero Jarque, L. Plaja, and L. Roso, Springer Series in Chemical Physics Vol. 100 (Springer, New York, 2011), Chap. 7, p. 145

Principles of SFA+

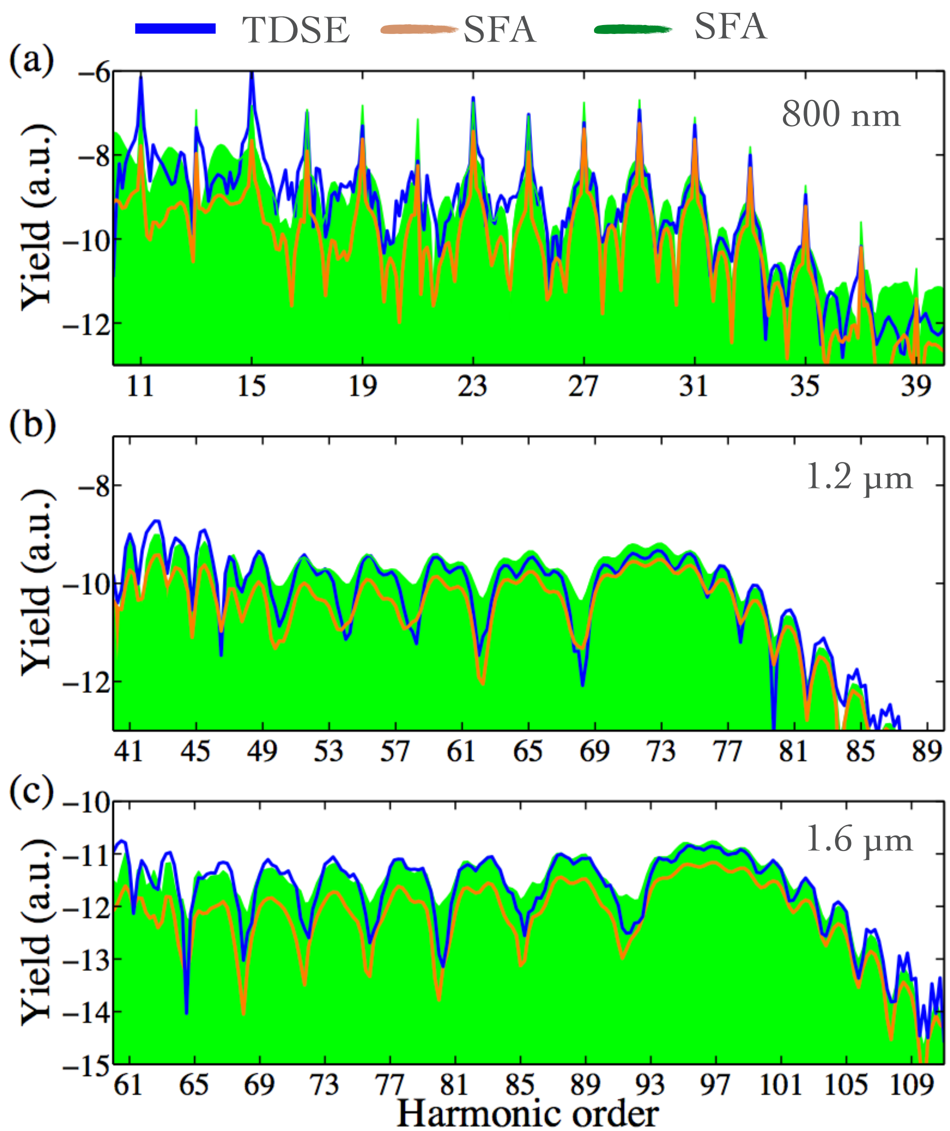

SFA+ with transversal saddle-point

$$\nabla_{k_\rho} S(\mathbf{k}, t, t_1) = 0$$

$$S(\mathbf{k}, t, t_1) \simeq S(k_z, k_\rho^{st}, t, t_1) + \frac{\hbar^2}{2m}(t - t_1) k_\rho^2$$

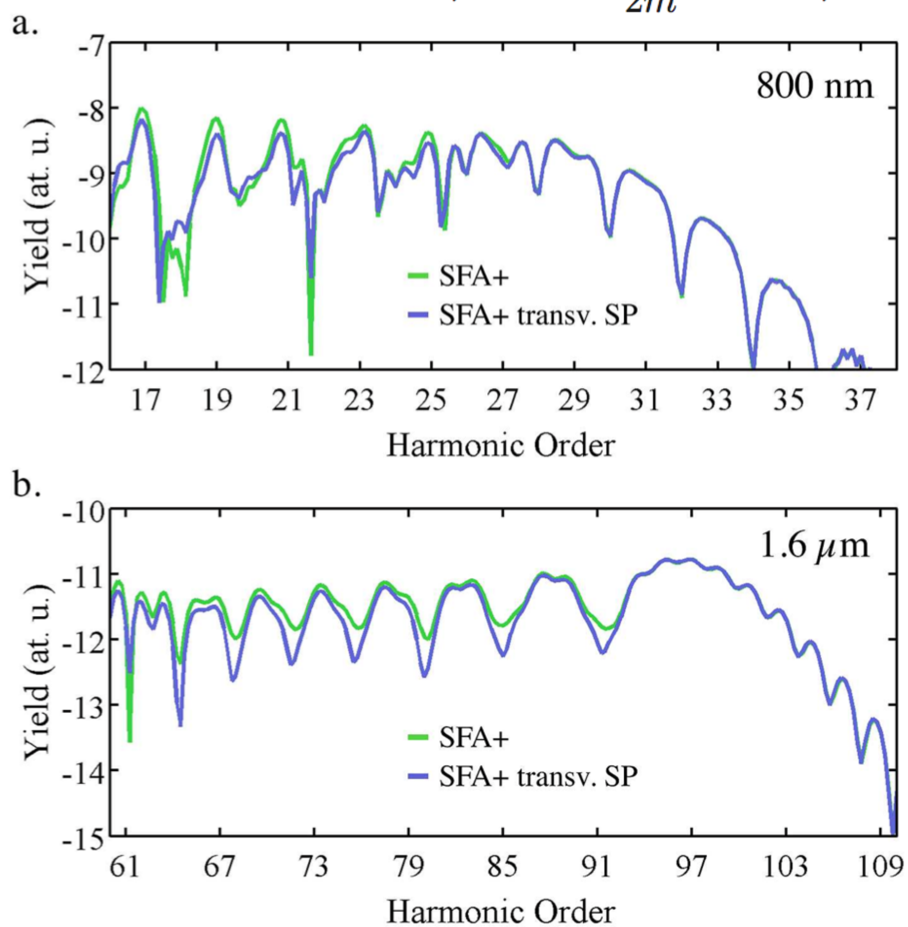

J.A. Pérez-Hernández, L. Roso and L. Plaja, Opt. Express 17, 9891 (2009)

C. Hernández-García, Doctoral dissertation (2013)

Obtaining X-rays from HHG

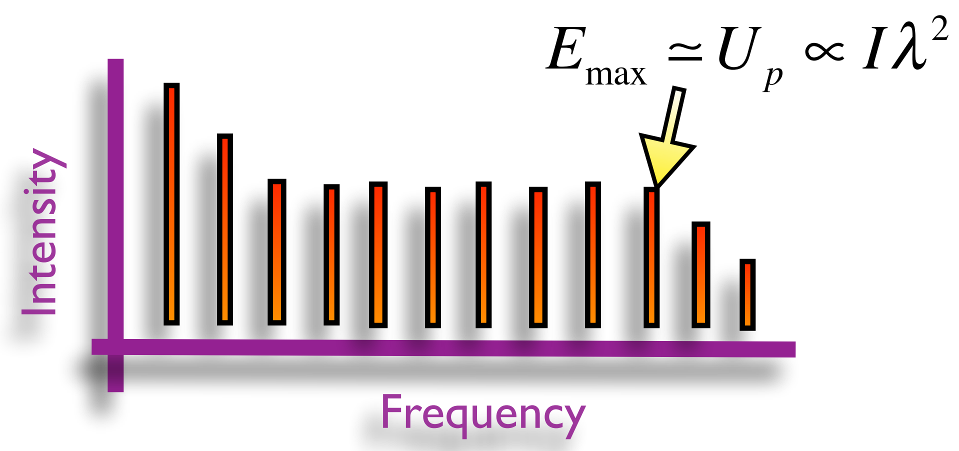

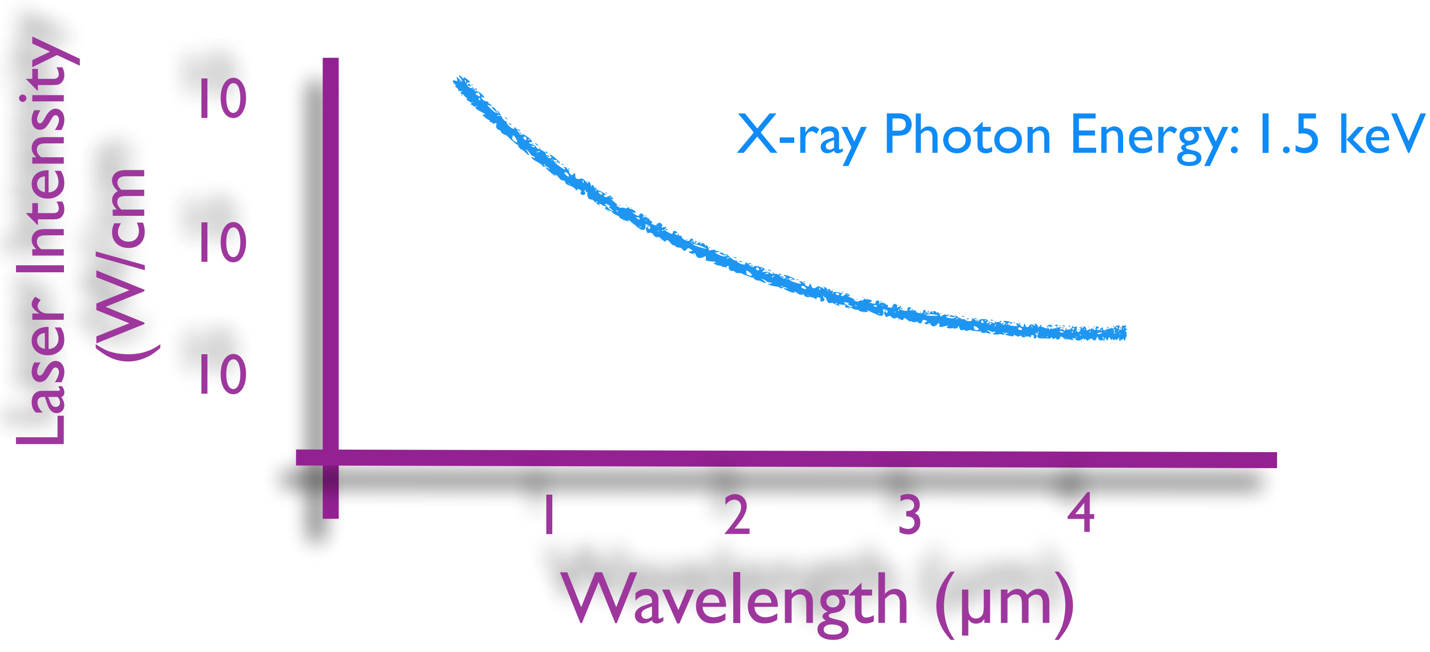

Unfavorable yield scaling law with wavelength

HHG yield scaling law $\lambda^{-5} - \lambda^{-6}$

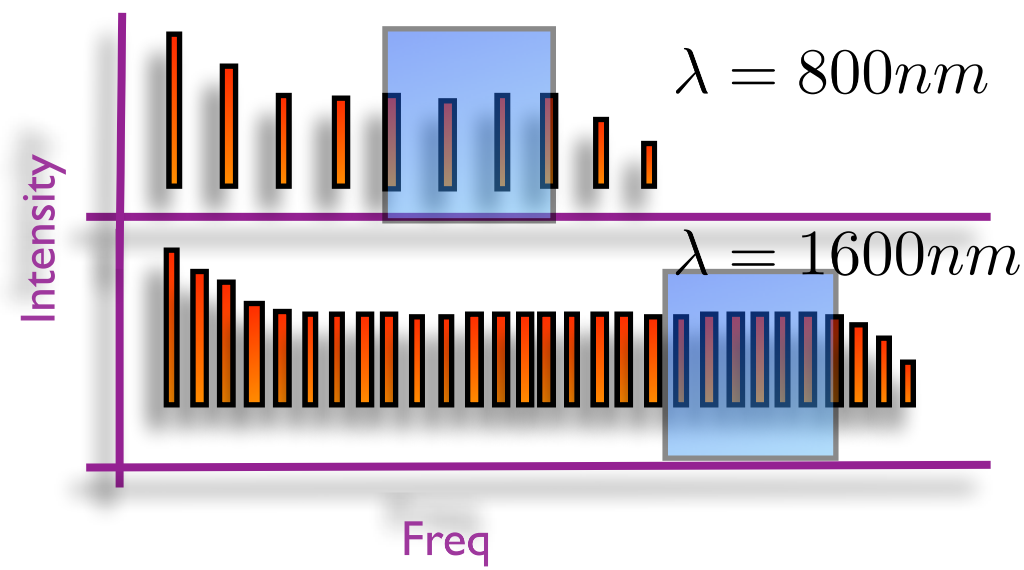

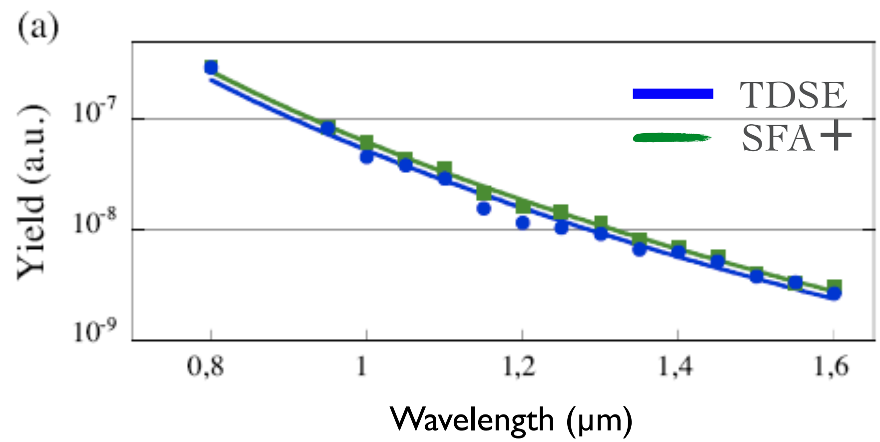

J. L. Tate, T. Auguste, H. G. Muller, P. Salières, P. Agostini, and L. F. DiMauro, PRL 98, 013901 (2007)
K. Schiessl, K.L. Ishikawa, E. Person, and J. Burgdörfer, PRL 99, 253903 (2007)
M.V. Frolov, N.L. Manakov, and A. Starace, PRL 100, 173001 (2008)
J.A. Pérez-Hernández, L. Roso and L. Plaja, Opt. Express 17, 9891 (2009)

Obtaining X-rays from HHG

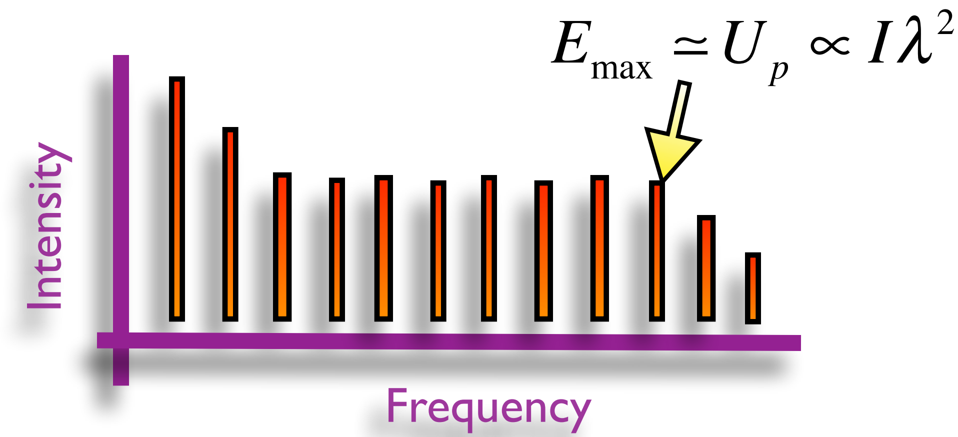

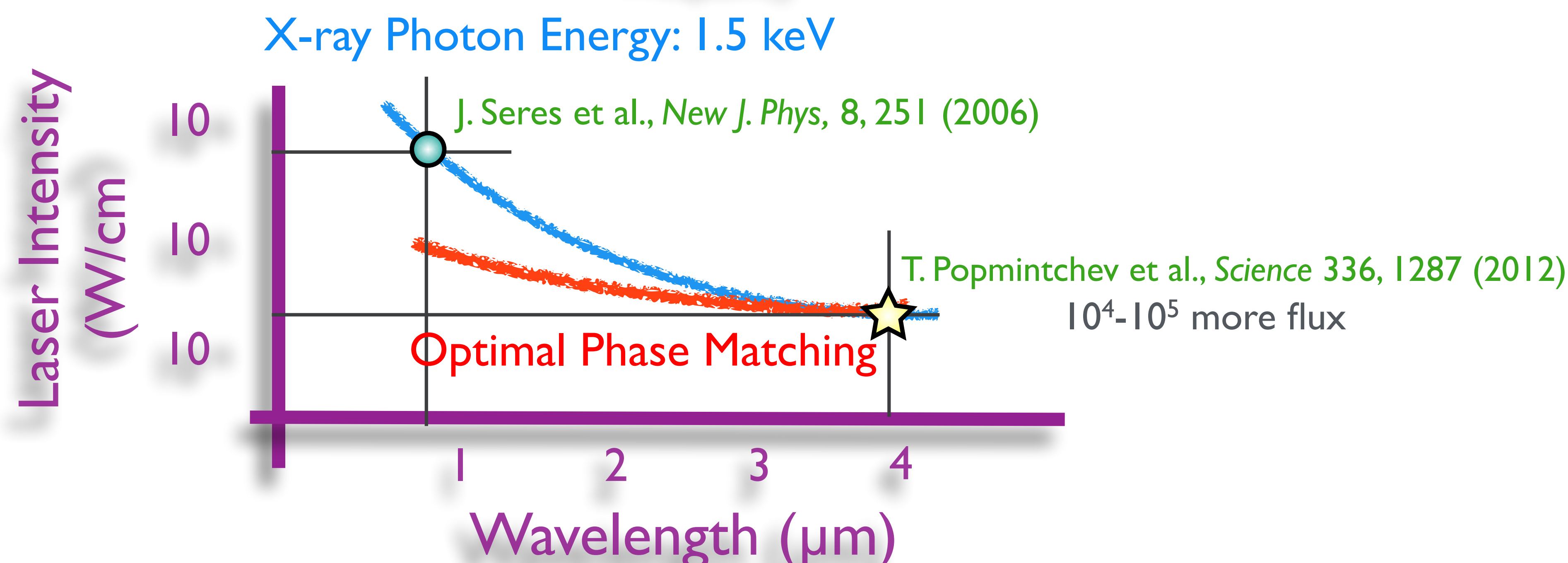

Phase-matched X-rays

Bright Coherent Ultrahigh Harmonics in the keV X-ray Regime from Mid-Infrared Femtosecond Lasers
Tenio Popmintchev *et al.*
Science **336**, 1287 (2012);
DOI: 10.1126/science.1218497

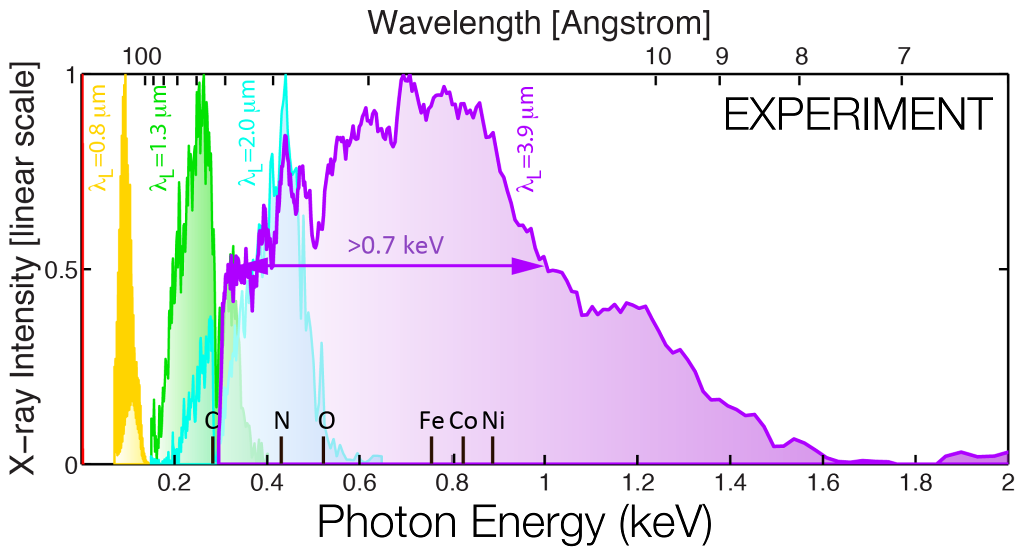

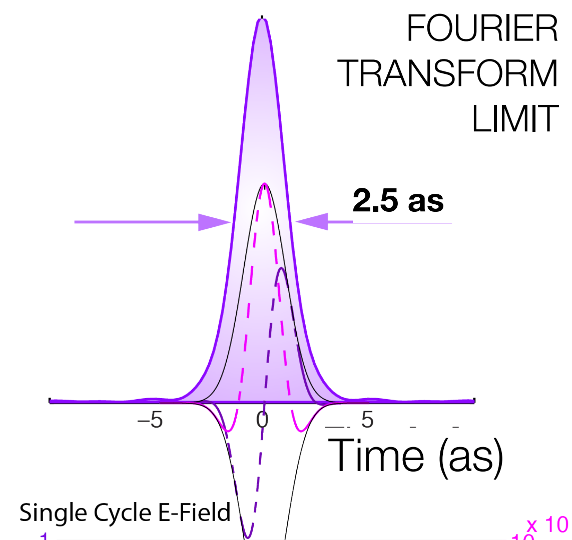

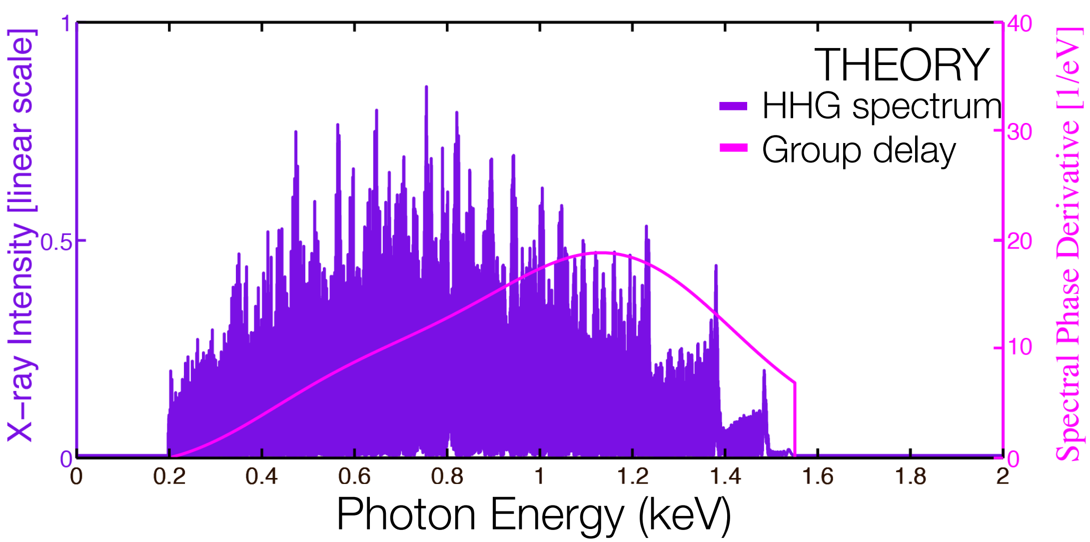

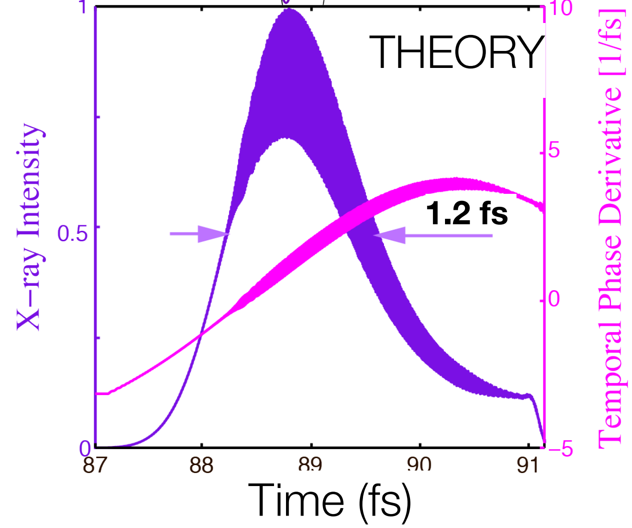

Single atom calculations at 4 µm

Laser field: $\lambda = 3.9\ \mu m$

$I = 3.6 \times 10^{14}\ W/cm^2$

$3\ cycles\ (38\ fs)$

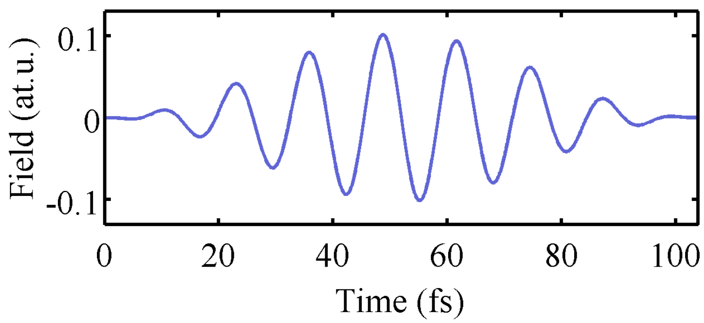

HHG spectrum

(SFA+ and transversal saddle point)

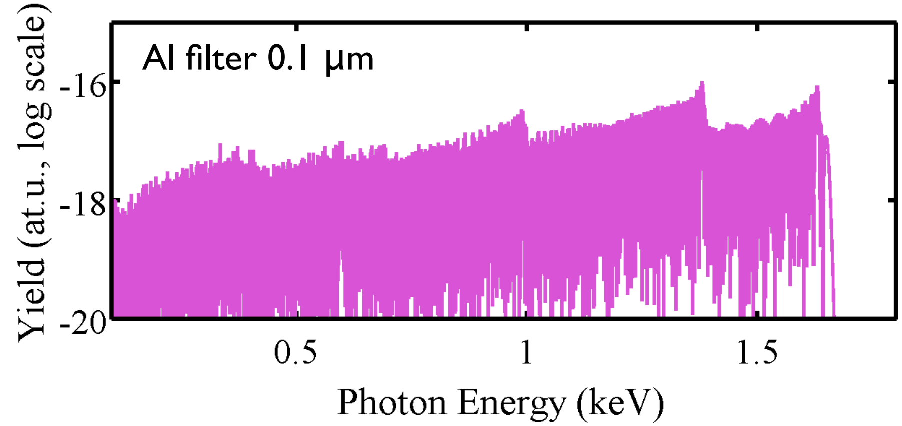

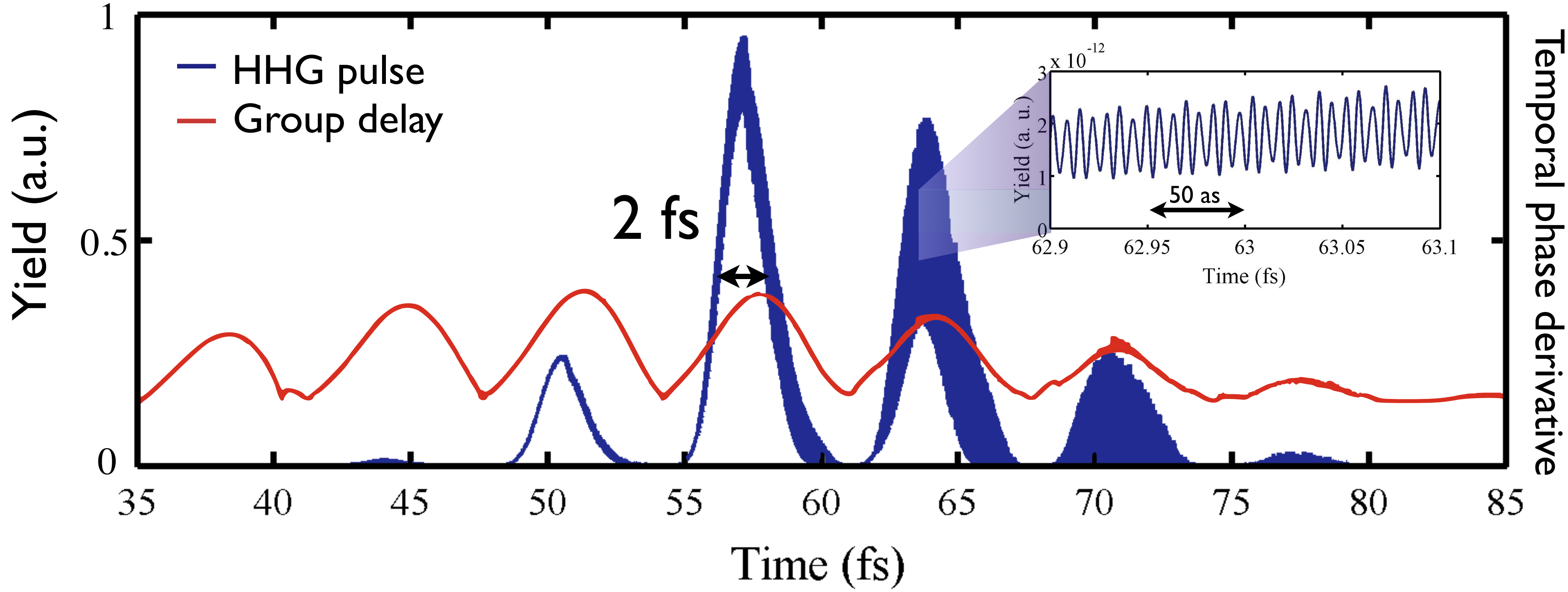

High-order rescattering effects

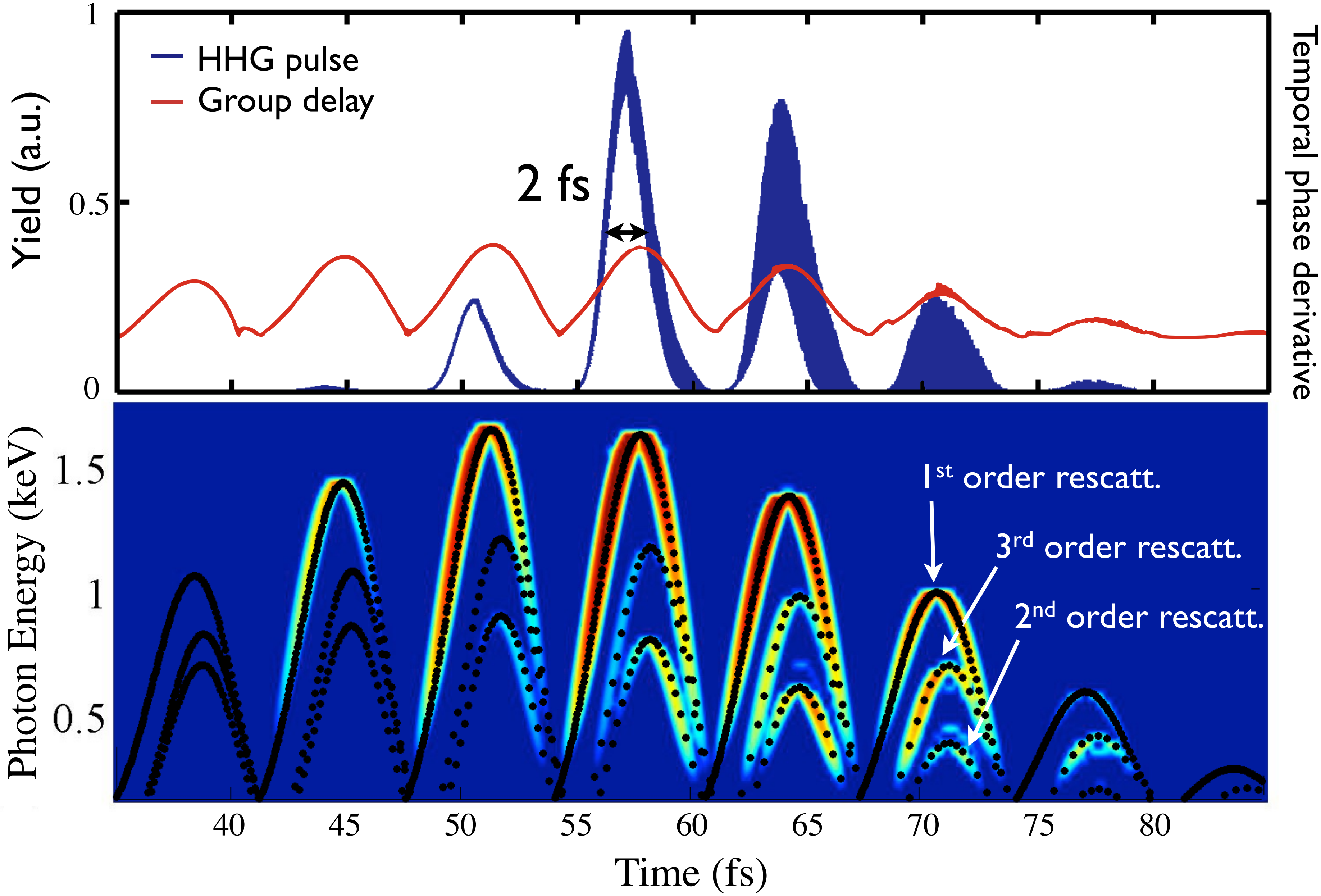

High-order rescattering effects

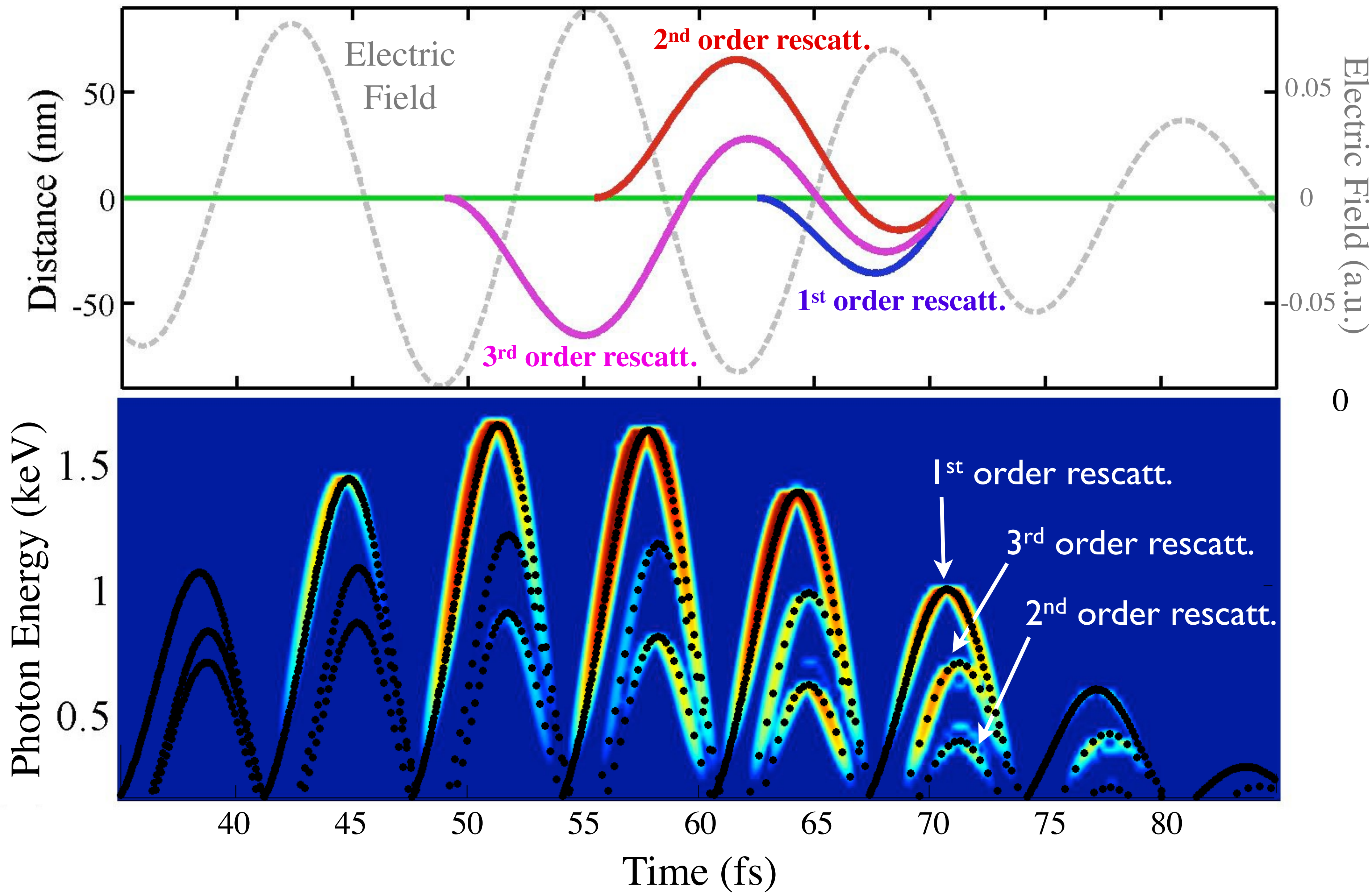

High-order rescattering effects

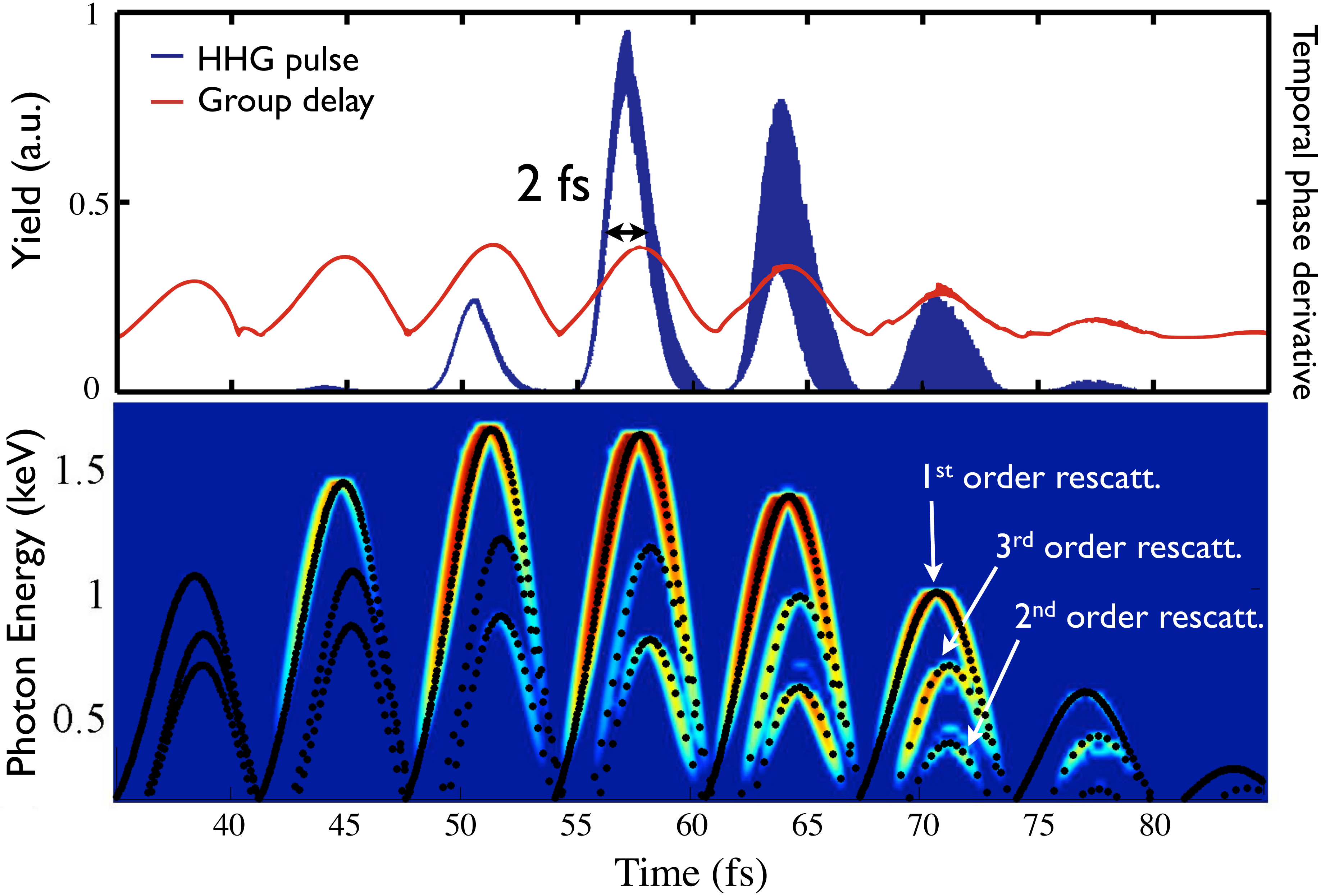

Attosecond pulse trains in the keV

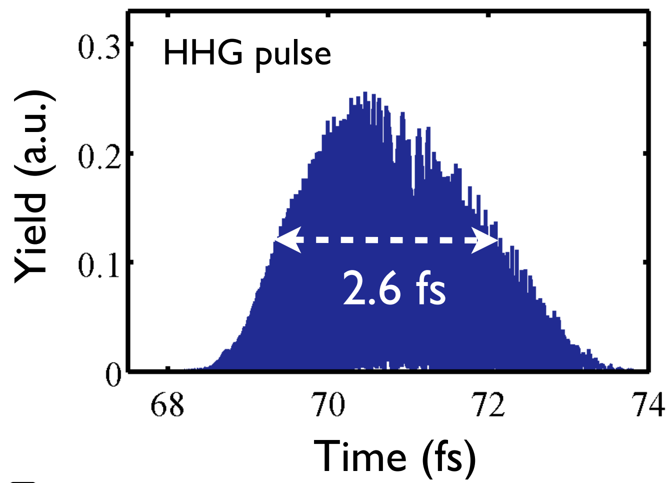

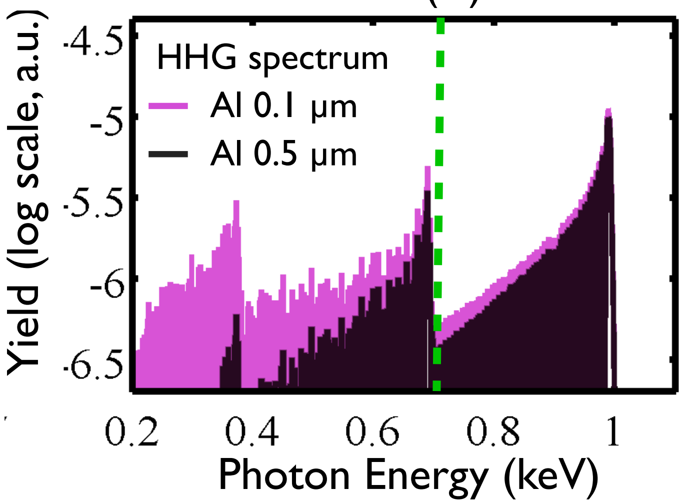

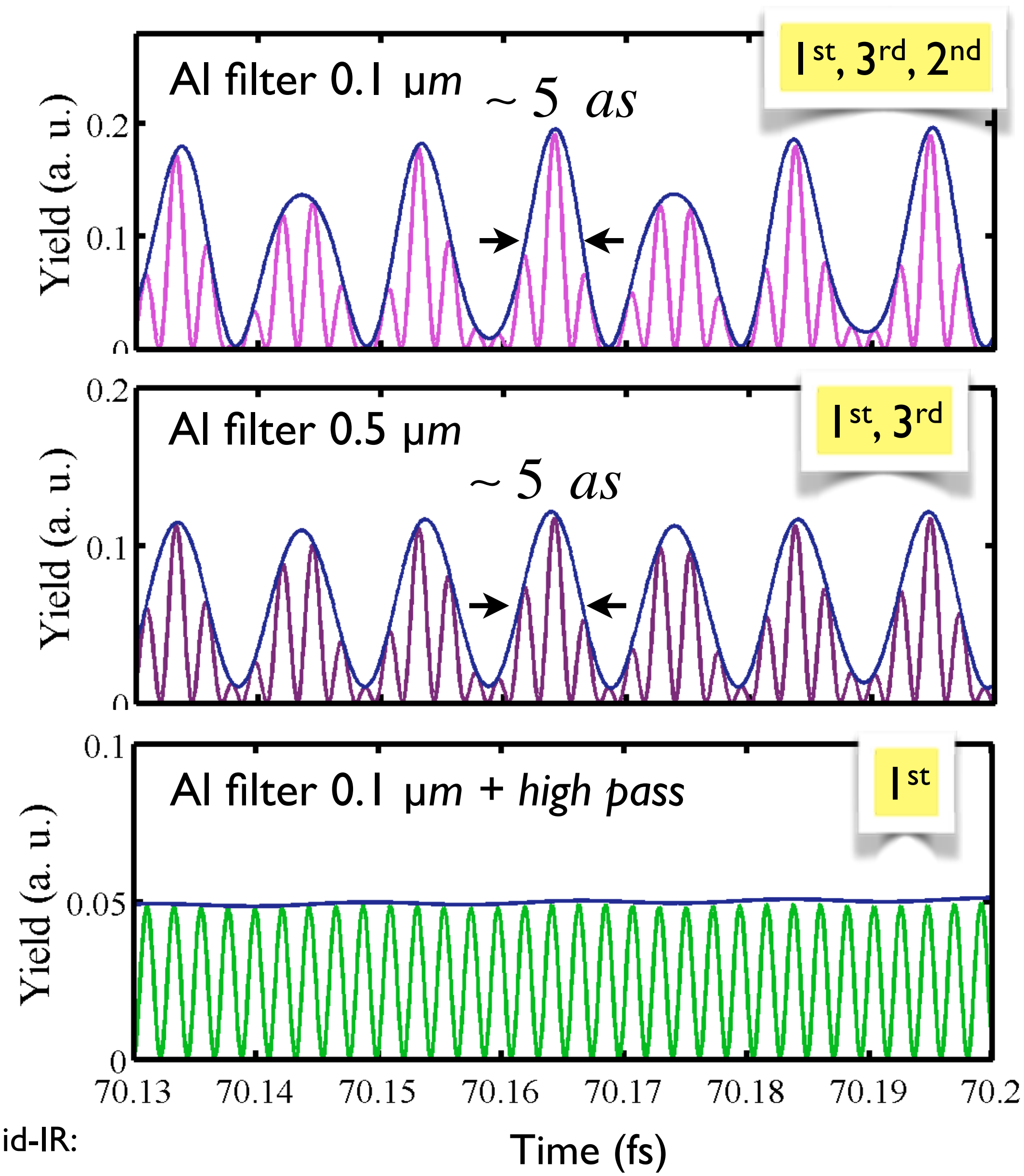

C. Hernández-García, J. A. Pérez-Hernández, T. Popmintchev, M. Murnane, H. Kapteyn, A. Jaron-Becker, A. Becker, and L. Plaja, PRL 111, 033002 (2013)

Previous works involving multiple rescatterings using mid-IR:

J. L. Tate, et al. PRL 98, 013901 (2007)

D. Hickstein et al. PRL 109, 073004 (2012)

Towards zeptosecond pulse trains

$$T = \frac{2\pi}{\Delta E}$$

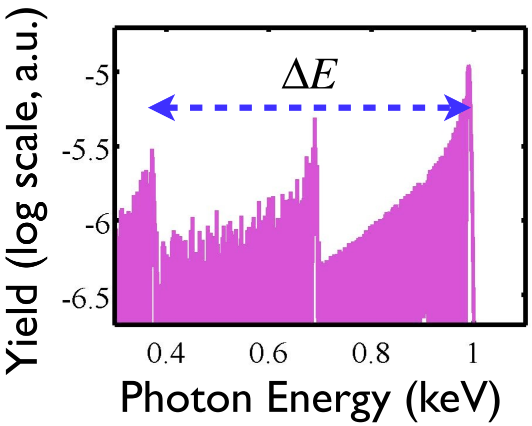

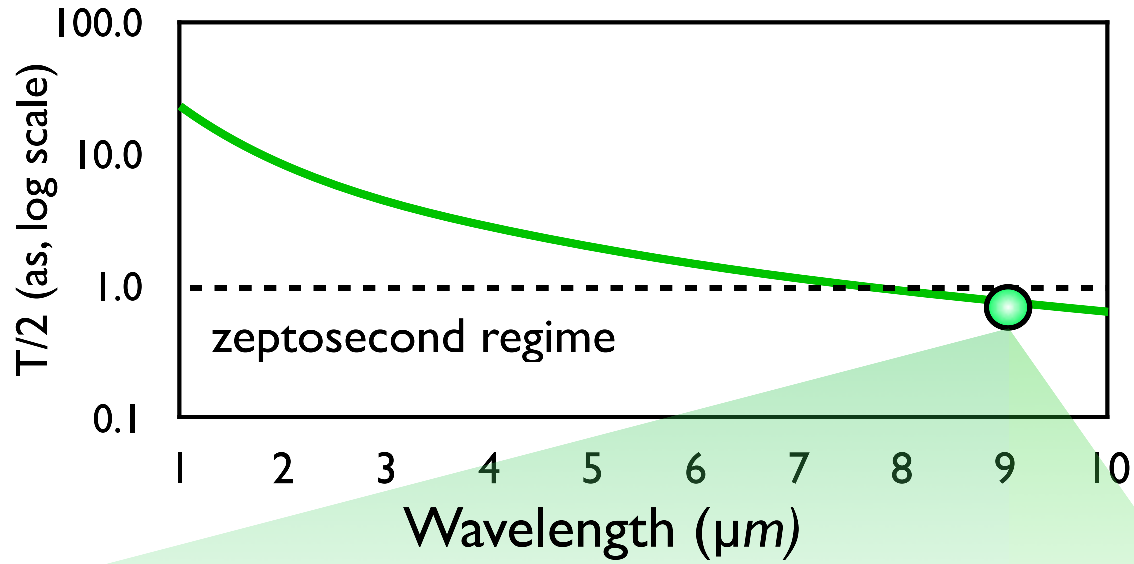

Laser field: $\lambda = 9\ \mu m$

$I = 3.16 \times 10^{14}\ W/cm^2$

$3\ cycles\ (90\ fs)$

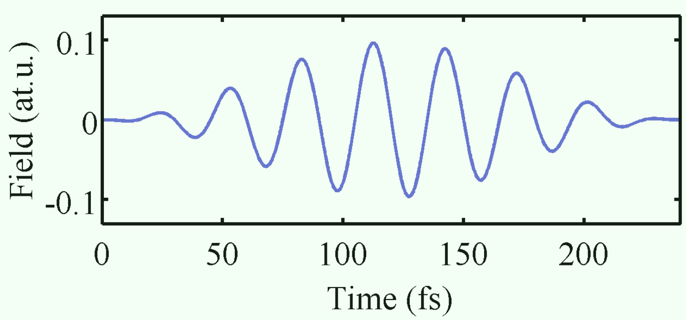

HHG spectrum (9 μm)

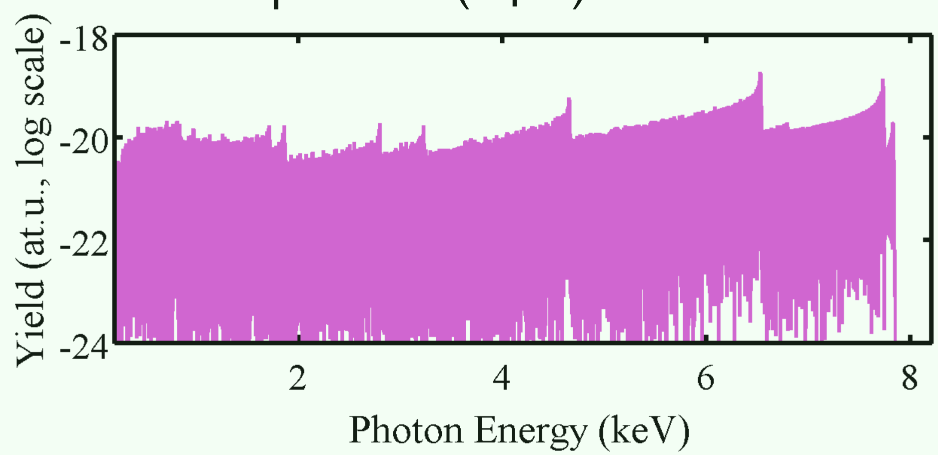

Towards zeptosecond pulse trains

$\lambda = 9 \ \mu m$

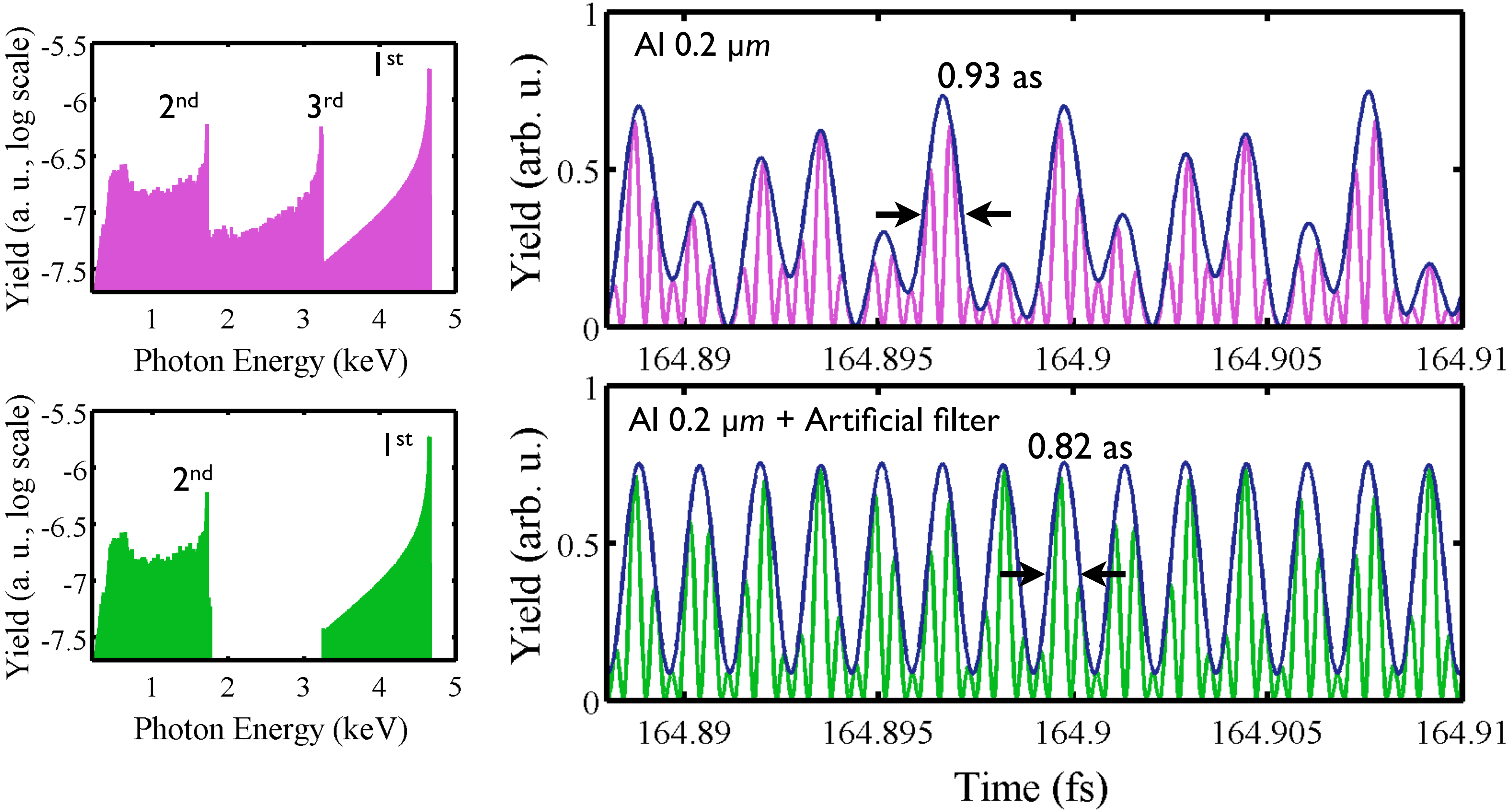

C. Hernández-García, J. A. Pérez-Hernández, T. Popmintchev, M. Murnane, H. Kapteyn, A. Jaron-Becker, A. Becker, and L. Plaja, Phys. Rev. Lett. 111, 033002 (2013)

Zeptosecond waveforms

$\lambda = 9\ \mu m$

Laser field: $I = 3.4 \times 10^{14}\ W/cm^2$

$1.44\ cycles\ (43 fs)$

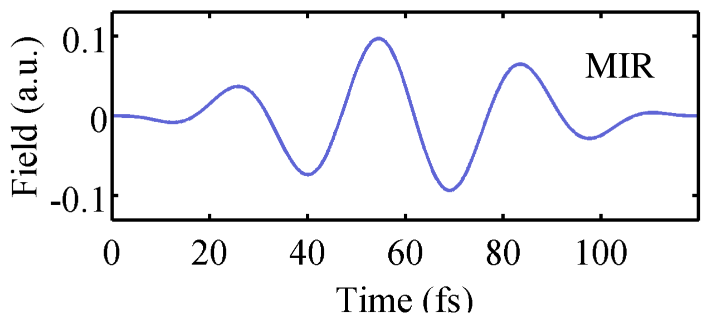

HHG spectrum

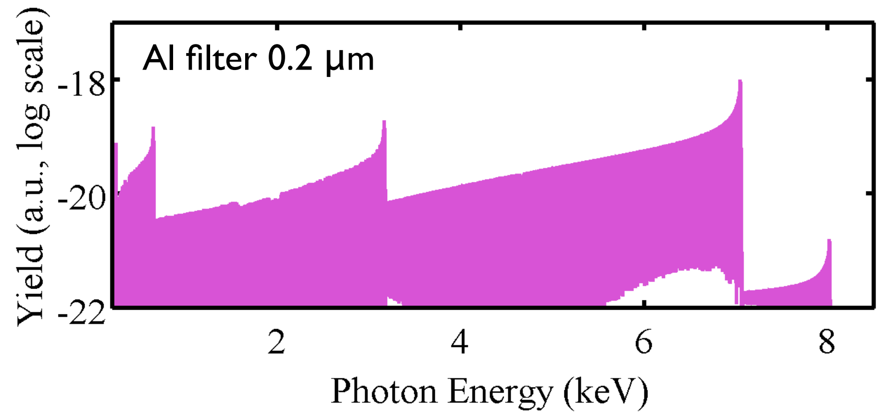

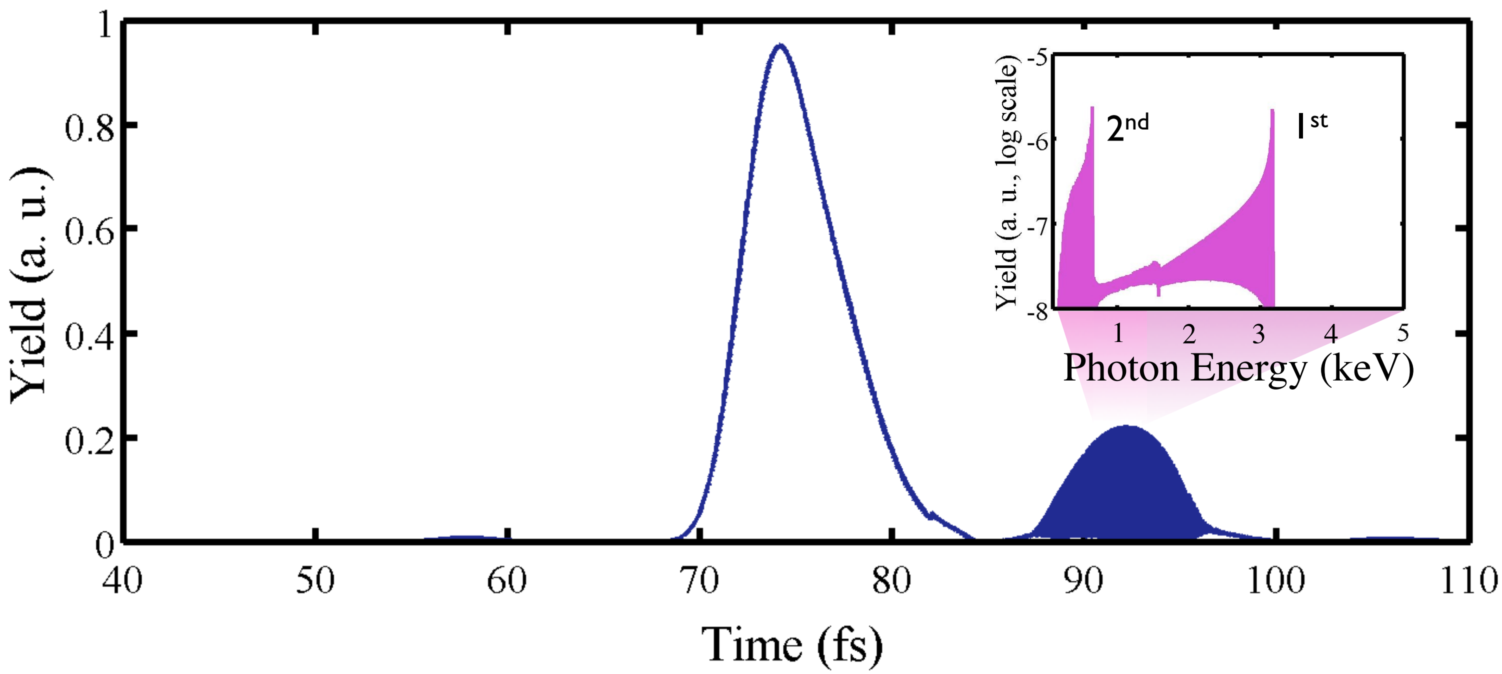

Zeptosecond waveforms

$$\lambda = 9\ \mu m$$

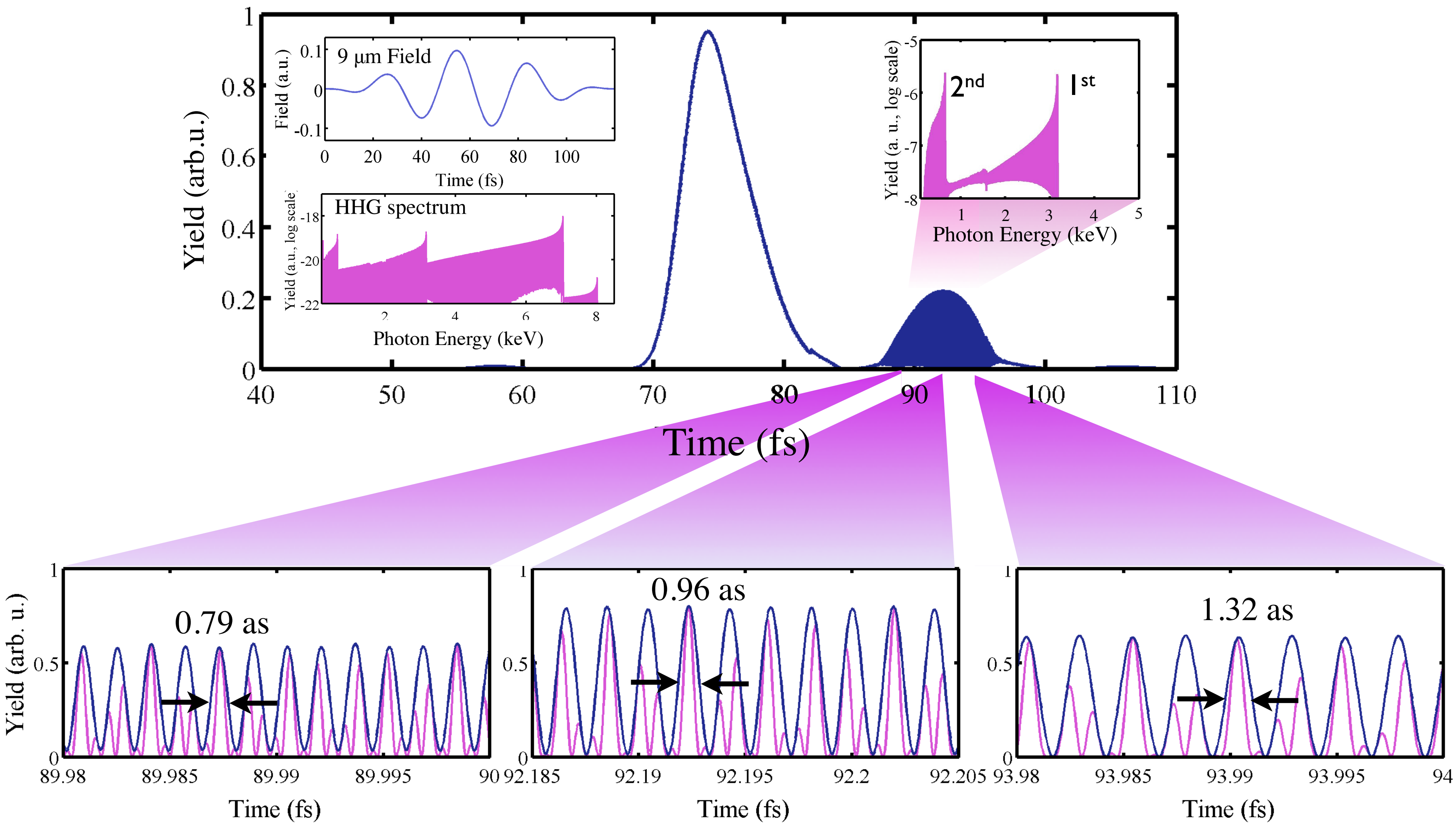

C. Hernández-García, J. A. Pérez-Hernández, T. Popmintchev, M. Murnane, H. Kapteyn, A. Jaron-Becker, A. Becker, and L. Plaja, Phys. Rev. Lett. 111, 033002 (2013)

Why not even longer wavelengths?

The magnetic drift mitigates the harmonic yield

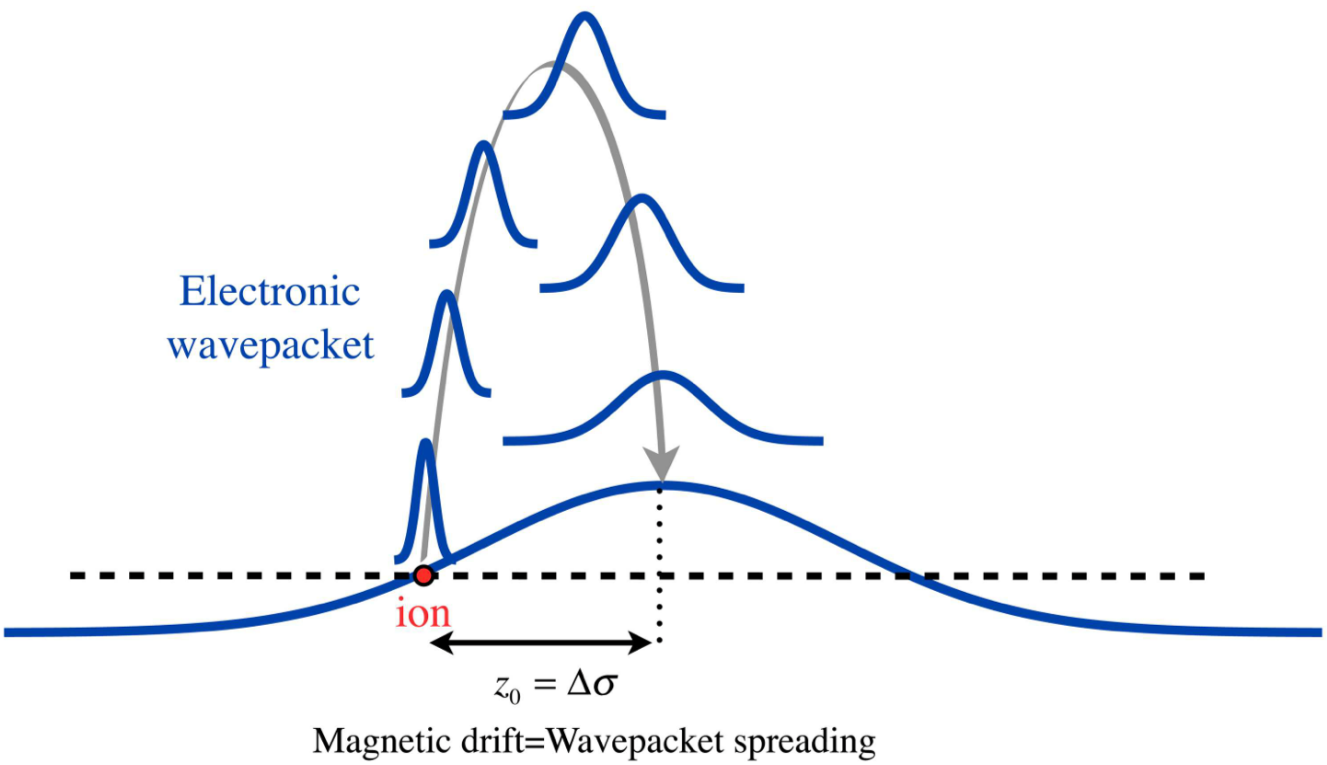

The yield would drop by an order of magnitude at 10 μm

C. Hernández-García, J. A. Pérez-Hernández, T. Popmintchev, M. Murnane, H. Kapteyn, A. Jaron-Becker, A. Becker, and L. Plaja, Phys. Rev. Lett. 111, 033002 (2013)

Macroscopic HHG

Phase-matching effects

Macroscopic Phase-matching

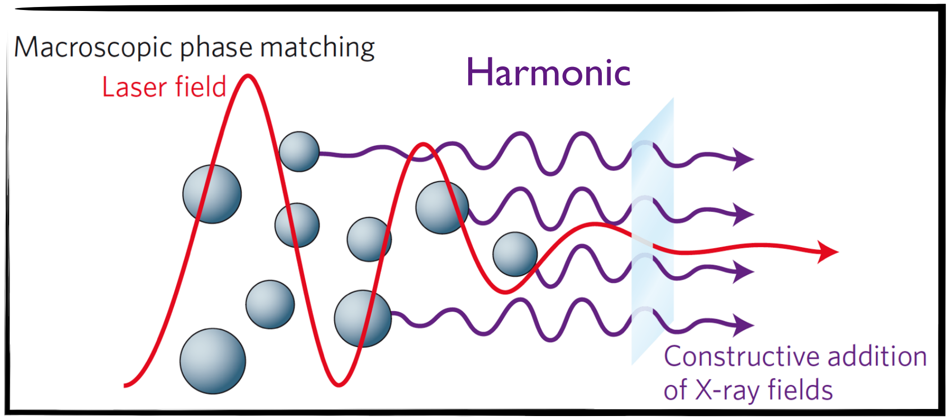

Figure courtesy of T. Popmintchev

Electric field of the qth-order harmonic:

$$E_q(\mathbf{r}) \propto \left[\left| d_q^j(\mathbf{r}) \right| e^{i\phi_q^j(\mathbf{r})} \right] e^{i(\mathbf{r}_d - \mathbf{r})\mathbf{k}_q}$$

$\left| d_q^j(\mathbf{r}) \right|$ spectral amplitude of the single-atom dipole, and

$\phi_q^j(\mathbf{r})$ its phase

Phase mismatch: $\Delta \mathbf{k}_q = \mathbf{k}_q - \nabla \phi_q^j = k_q \mathbf{e}_z - \frac{\partial \phi_q^j}{\partial z} \mathbf{e}_z - \frac{\partial \phi_q^j}{\partial \rho} \mathbf{e}_\rho$

Perfect phase-matching $\Delta k_q = 0$

$$\Delta k_q^{\parallel} = k_q - \frac{\partial \phi_q^j}{\partial z} \simeq q \frac{\omega}{c} \left[n_r(q\omega_0) - n_r(\omega_0) \right] + (q-1) \frac{\partial \zeta(z)}{\partial z} + \alpha_q^j \frac{\partial I(z)}{\partial z}$$

Longitudinal PM

$$\Delta k_q^{\perp} = -\frac{\partial \phi_q^j}{\partial \rho} \simeq -q \frac{\omega}{c} n_r(\omega) \frac{\rho}{R(z)} + \alpha_q^j \frac{\partial I(z)}{\partial z}$$

Transversal PM

C. Hernández-García, I.J. Sola, and L. Plaja, *Phys. Rev. A* 88, 043848 (2013)

Contributions to phase-matching

$$\Delta k_q = k_q - qk_1 \simeq \Delta k_q^{geom} + \Delta k_q^{\text{int}} + \Delta k_q^{f} + \Delta k_q^{b}$$

Geometrical: Gouy + angle of detection

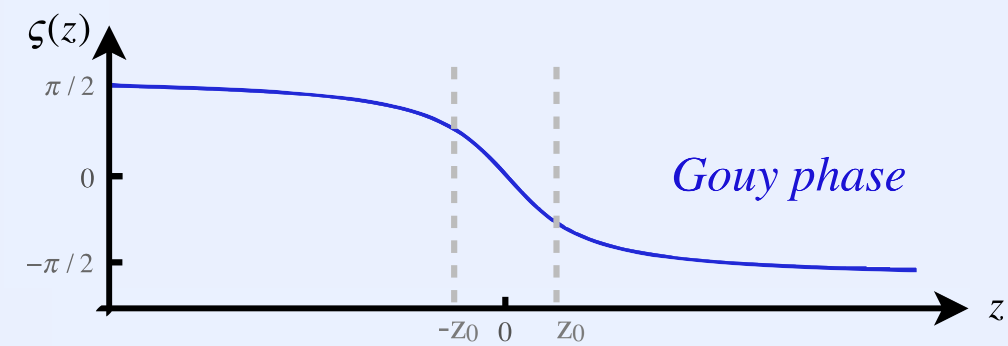

$$\Delta k_q^{geom} \approx \frac{q-1}{z_0} - \frac{q\omega_0}{2c}\theta^2$$

Intrinsic phase

$$\phi_q^i = \frac{1}{\hbar} S\left(\vec{k}^{st}, t^{st,i}, t_{ion}^{st,i}\right) + \omega t^{st,i} \qquad \Delta k_q^{\text{int}} \approx \alpha_q^i \frac{\partial I(z)}{\partial z}$$

Free electrons and neutrals

$$n_r \simeq 1 + 2\pi\left(\chi_f + \chi_b\right)$$

$$\Delta k_q^{f,b} = \frac{4\pi^2}{\lambda_q}\left[\chi_{f,b}(\lambda_q) - \chi_{f,b}(\lambda_0)\right] \simeq \frac{4\pi^2}{\lambda_q}\chi_{f,b}(\lambda_0)$$

Computing Harmonic Propagation

1) The **standard way**: to solve the Wave equation

$$\nabla^2 \vec{E} - \frac{1}{c^2}\frac{\partial}{\partial t^2}\vec{E} = \frac{4\pi}{c^2}\frac{\partial}{\partial t}\vec{J}$$

A. L'Huillier et al, J. Opt. Soc. Am. B 7, 527 (1990).
A. L'Huillier, et al, Phys. Rev. A 46, 2778 (1992).

✓ Slowly Varying Envelope Approximation: $\partial^2/\partial t^2 \ll \omega\,\partial/\partial t$

✓ Paraxial Approximation: $\partial^2/\partial z^2 \ll k\,\partial/\partial z$

2) **Our choice**: to use the formal solution of the Maxwell's equations for an elementary radiator:

$$\vec{E}_i(\vec{r},t) = -\frac{1}{c^2}\int d\vec{r}\,'\frac{1}{|\vec{r}-\vec{r}\,'|}\left[\frac{\partial}{\partial t'}\vec{J}(\vec{r}\,',t')\right]_{ret}$$

without Slowly Varying Envelope and Paraxial Approximations.

C. Hernández-García, et al, Phys. Rev, A 82, 0033432 (2010)

Sum of elementary radiators

We decompose the integral into a discrete sum of elementary contributions:

$$\vec{E}_i^j(\vec{r},t) = -\frac{1}{c^2}\sum_{j=1}^{N}\frac{q_j}{\left|\vec{r}-\vec{r}_j(0)\right|}\vec{s}_d \times \left(\vec{s}_d \times \vec{a}_j\left(t-\left|\vec{r}-\vec{r}_j(0)\right|/c\right)\right)$$

Discrete Dipole Approximation

reduces from 10^{12} to 10^5 radiators

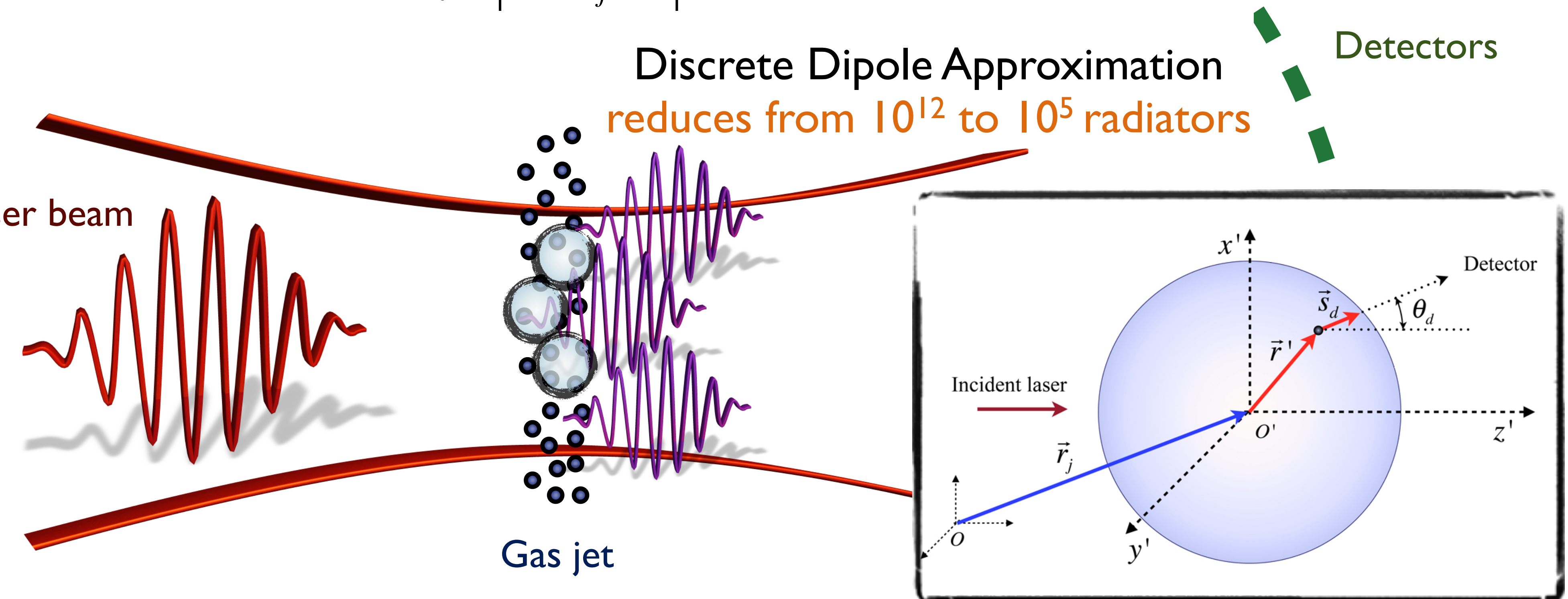

C. Hernández-García, J.A. Pérez-Hernández, J. Ramos, E. Conejero Jarque, L. Roso, and L. Plaja, Phys. Rev, A 82, 0033432 (2010)

$$\vec{E}_{i,j}(\vec{r}_d,\omega) \propto -N(\vec{r}_j)\vec{s}_d \times \left(\vec{s}_d \times \vec{a}_j\left(\vec{r}_j,\omega\right)e^{-i\frac{\omega}{c}\left|\vec{r}_d-\vec{r}_j\right|}F(\theta_d,\omega)\right)$$

DDA - Convergence

Without DDA ← With DDA →

Point Atoms

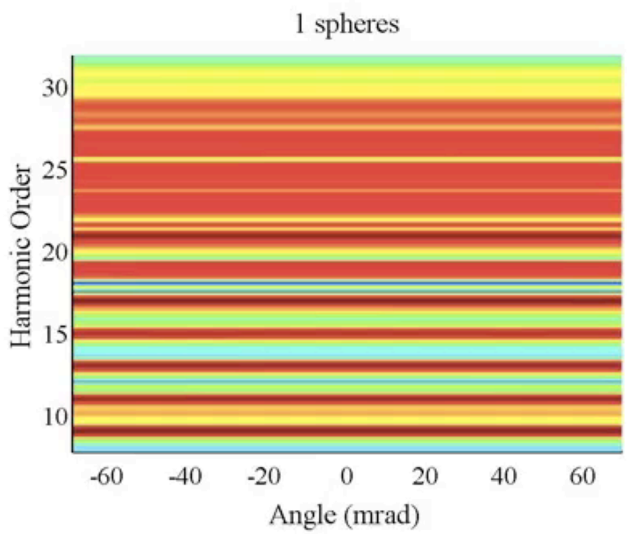

1 μm Spheres

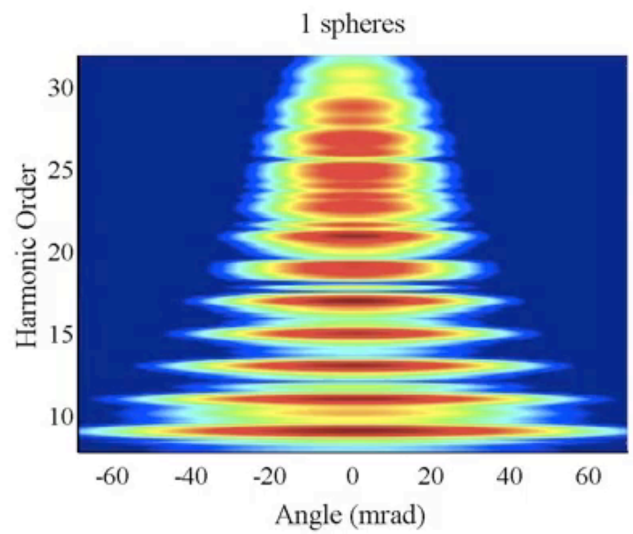

2 μm Spheres

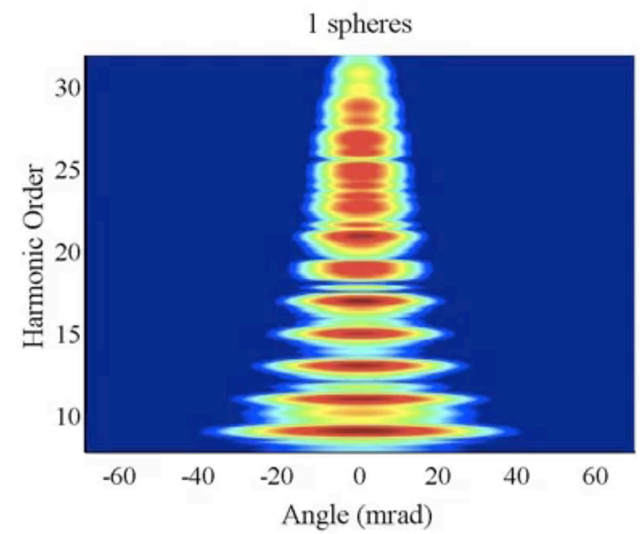

C. Hernández-García, J.A. Pérez-Hernández, J. Ramos, E. Conejero Jarque, L. Roso, and L. Plaja, Phys. Rev, A 82, 0033432 (2010)

On-axis phase-matching in a gas jet

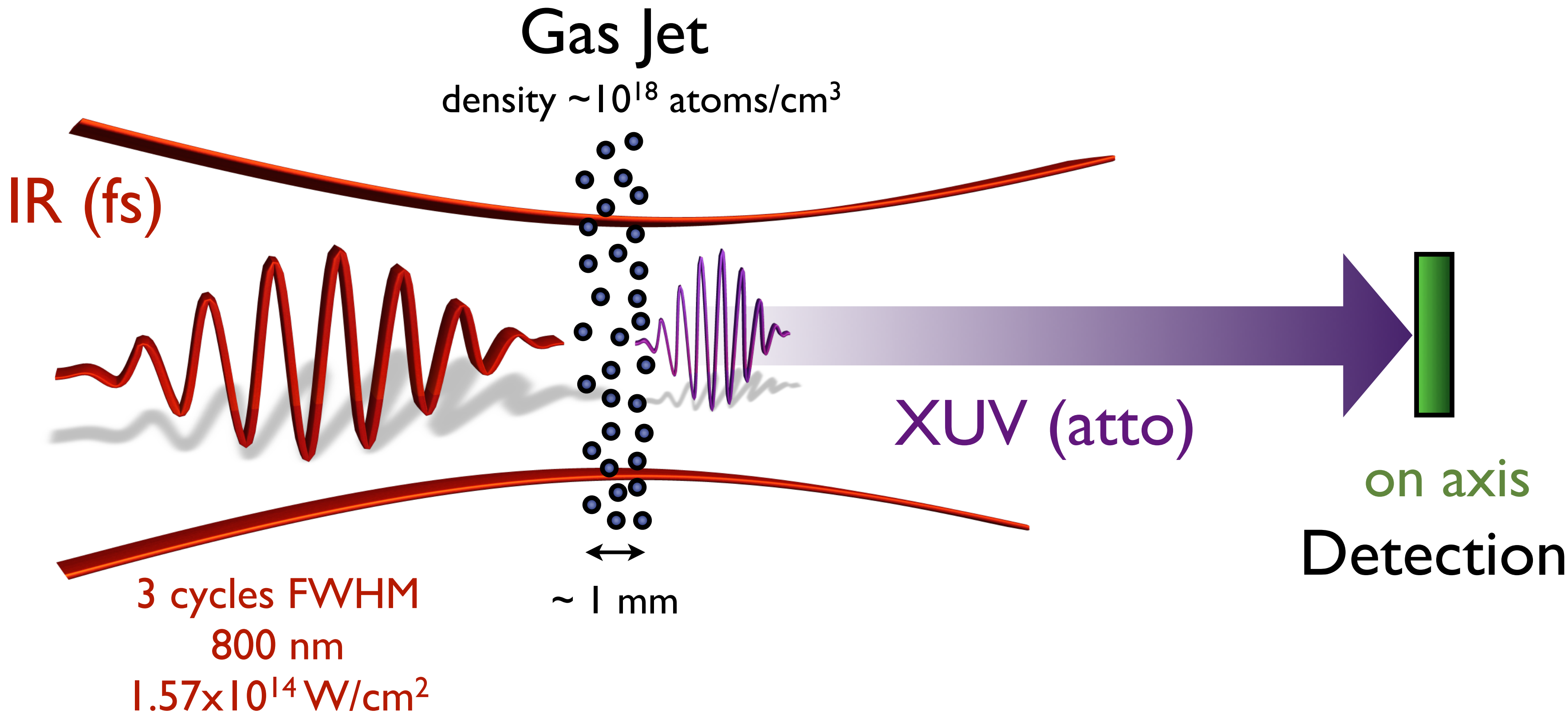

$$\Delta k_q \simeq \Delta k_q^{Gouy} + \Delta k_q^{\text{int}} + \Delta k_q^{f} + \Delta k_q^{b} \simeq \frac{q-1}{z_0} + \alpha_q^i \frac{\partial I(z)}{\partial z} + q\frac{e^2 n_f \lambda_0}{mc^2}$$

On-axis phase-matching in a gas jet

$$\Delta k_q \simeq \Delta k_q^{Gouy} + \Delta k_q^{\mathrm{int}} + \Delta k_q^{f} + \Delta k_q^{b} \simeq \frac{q-1}{z_0} + \alpha_q^i \frac{\partial I(z)}{\partial z} + q\frac{e^2 n_f \lambda_0}{mc^2}$$

before the focus >0 >0

after the focus >0 <0

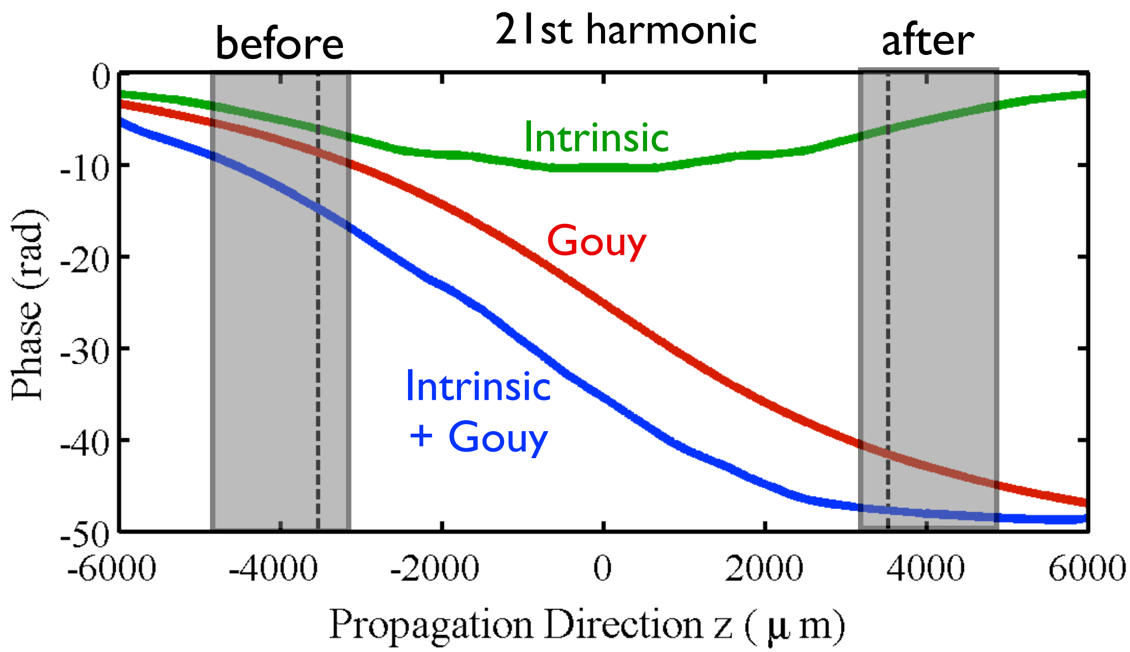

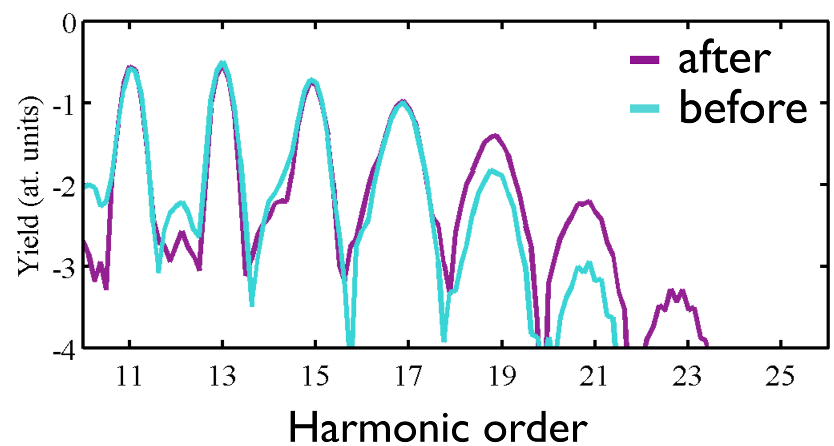

Already demonstrated:

P. Salières, A. L'Huillier, and M. Lewenstein, PRL, 74, 3776 (1995)
P. Antoine , A. L'Huillier, and M. Lewenstein, PRL, 77, 1234 (1996)
M. B. Gaarde, J. L. Tate, and K.J. Schafer J. Phys. B: At. Mol. Opt. Phys. 41 (2008)

Off-axis phase-matching in a gas jet

$$\Delta k_q \simeq \Delta k_q^{Gouy} + \Delta k_q^{\text{int}} + \Delta k_q^{f} + \Delta k_q^{angle} \simeq \frac{q-1}{z_0} + \alpha_q^i \frac{\partial I(z)}{\partial z} + q\frac{e^2 n_f \lambda_0}{mc^2} - \frac{q\omega_0}{2c}\theta^2$$

Before the focus

After the focus

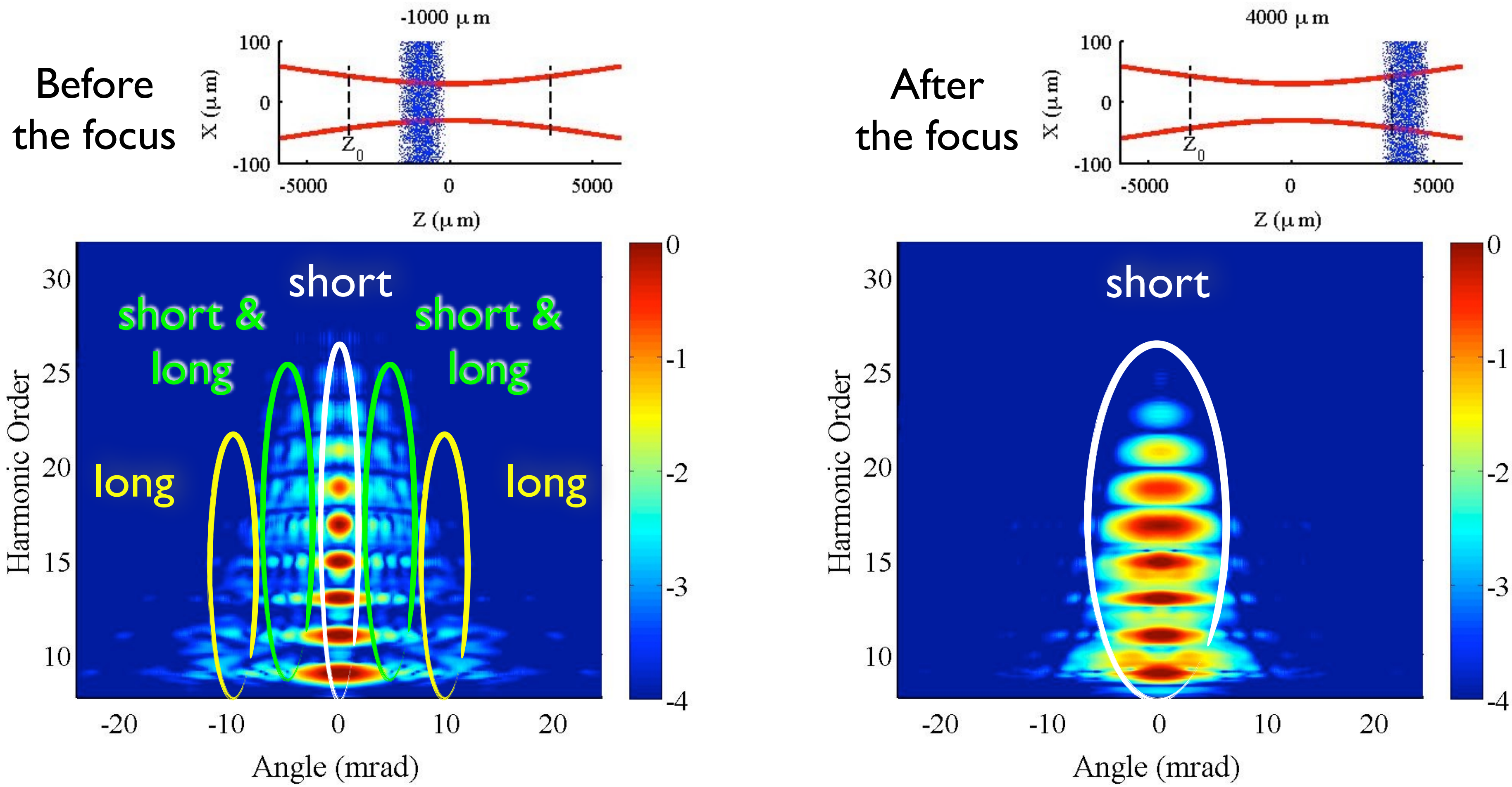

Deliverables of our Phase-matching code

Experimental comparisons

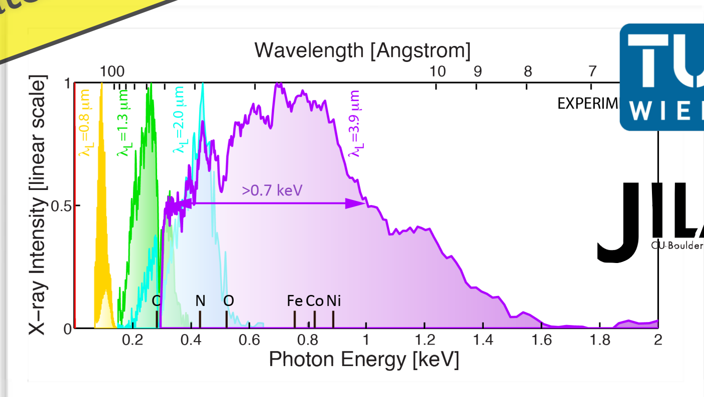

1.6 keV HHG X-rays

T. Popmintchev, et al *Science* 336, 1287 (2012)

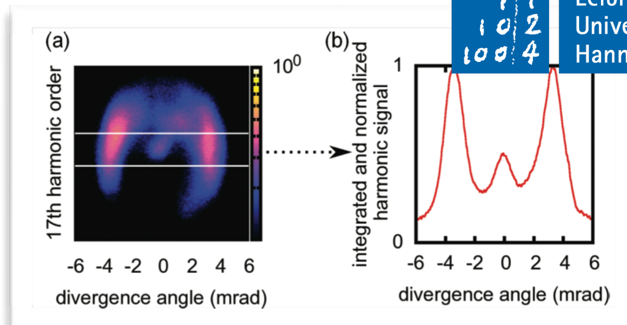

XUV harmonics in gas cell

M. Kretschmar, et al. Phys. Rev. A 88, 013805 (2013)

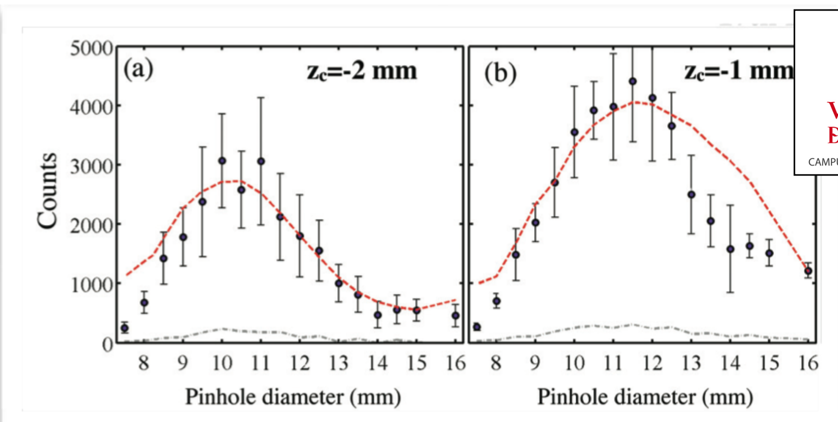

Role of transversal phase-matching

C. Hernández-García, et al Phys. Rev. A 88, 043848 (2013)

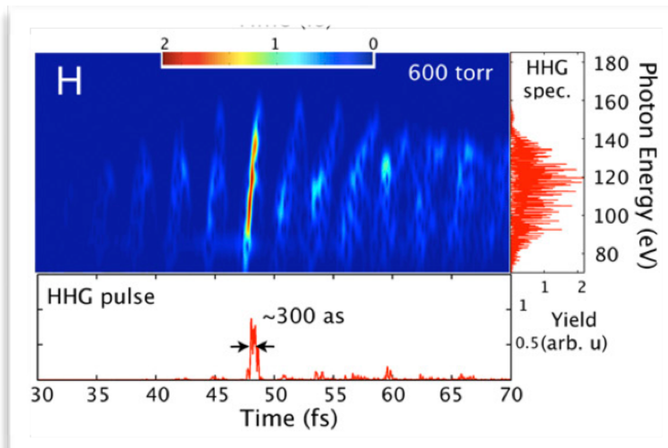

Isolated X-ray attosecond pulses

M.-C. Chen, et al PNAS 111, E2361-E2367 (2014)

XUV harmonics from few-cycle pulses

W. Holgado et. al. (in preparation) (2014)

Deliverables of our Phase-matching code

New theoretical findings

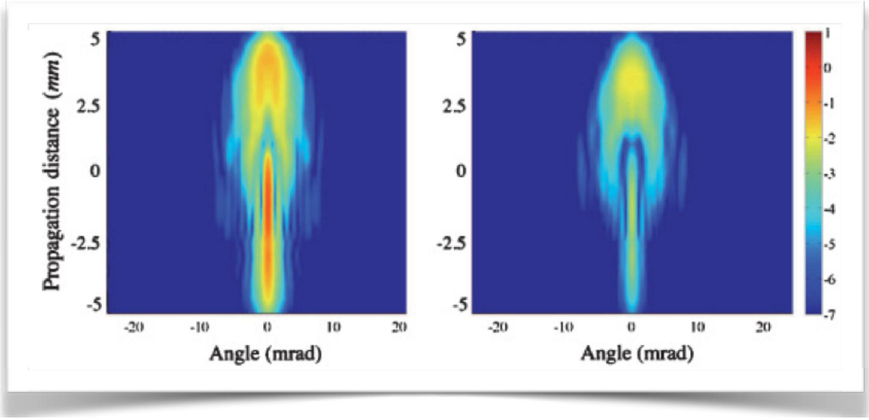

Phase-matching conditions along the propagation direction

C. Hernández-García, et al, Phys. Rev, A 82, 0033432 (2010)

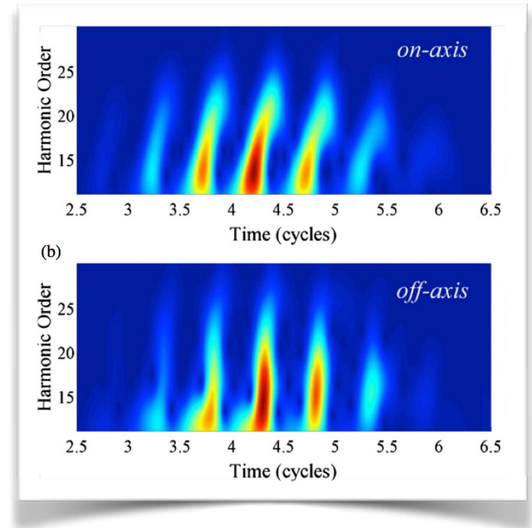

Off-axis compensation of the atto-chirp

C. Hernández-García, and L. Plaja, J. Phys. B: At. Mol. Opt. Phys. 45, 074021 (2012)

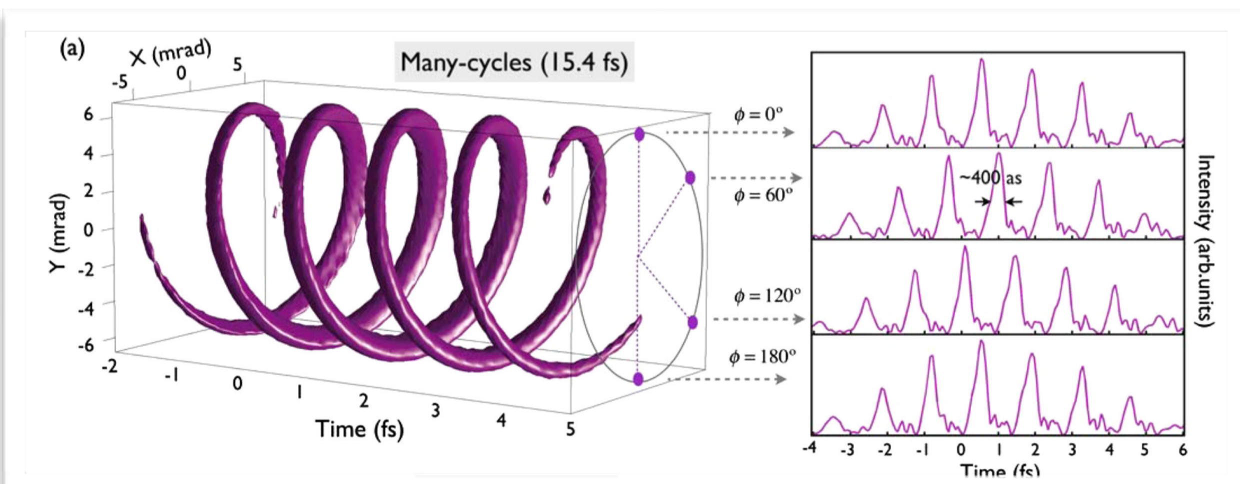

XUV vortices: conservation of orbital angular momentum (OAM) in HHG

C. Hernández-García, A. Picón, J. San Román , and L. Plaja, Phys. Rev. Lett. 111, 083602 (2013)

Isolating an attosecond pulse

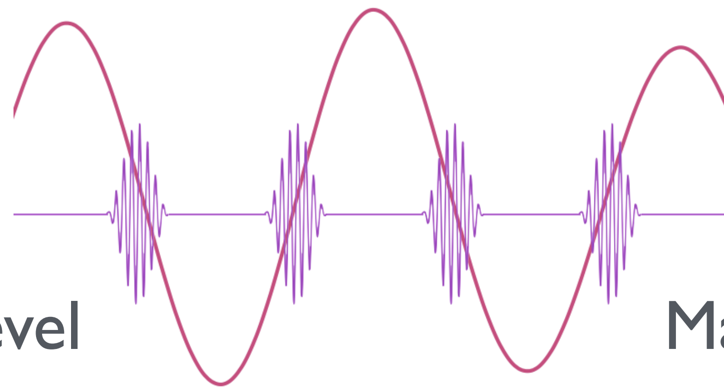

Microscopic level

Macroscopic level

Single Event

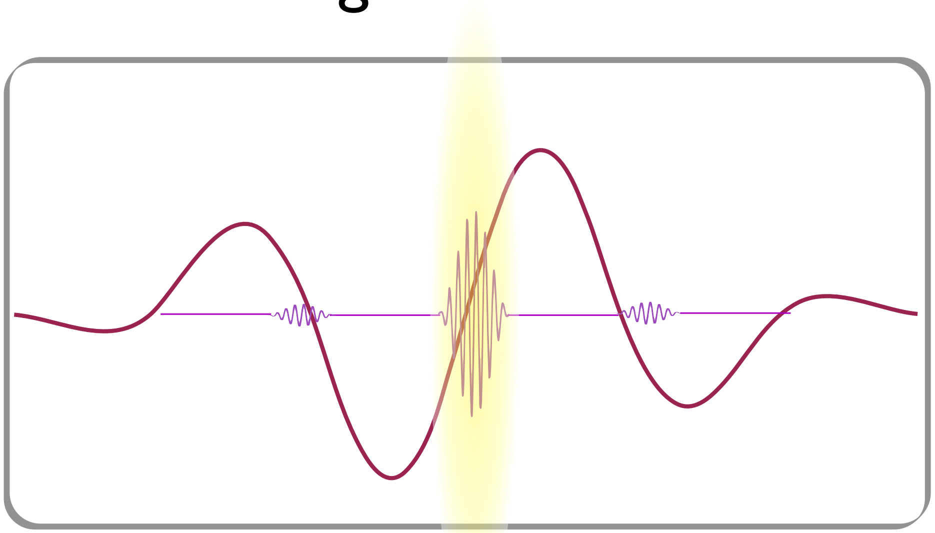

E. Goulielmakis et al., *Science* **320**, 1614–1617 (2008).
B.Shan et al., *J. Mod. Opt.* **52**, 277 (2005).
I. J. Sola *et al.*, *Nature Physics* **2**, 319–322 (2006).
G. Sansone et al., *Science* **314**, 443–446 (2006).
E. J. Takahashi, et al., *Phys. Rev. Lett.* **104**, 233901 (2010).
Zhao et al. Opt. Lett. 37, 3891 (2012)

Phase-matching Isolation

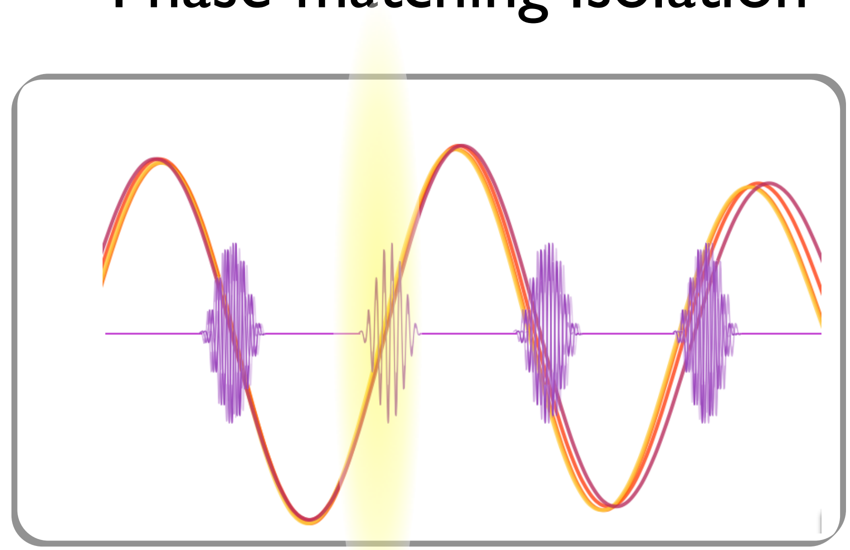

M. J. Abel et al., Chem Phys **366**, 9–14 (2009)
I. Thomann et al.,*Opt.Express* **17**, 4611 (2009)
F. Ferrari, F. Calegari, M. Lucchini, C. Vozzi, S. Stagira, G. Sansone, and M. Nisoli, Nature Photonics 4, 875–879 (2010)
M.-C. Chen, C. Mancuso, C. Hernández-García, F. Dollar, B. Galloway, D. Popmintchev, B. Langdon, A. Auger, P.-C. Huang, B.C. Walker, L. Plaja, A. Jaron-Becker, A. Becker, M. M. Murnane, H. C. Kapteyn, T. Popmintchev, PNAS 111 (23) , E2361-E2367 (2014)

Optimal phase-matching

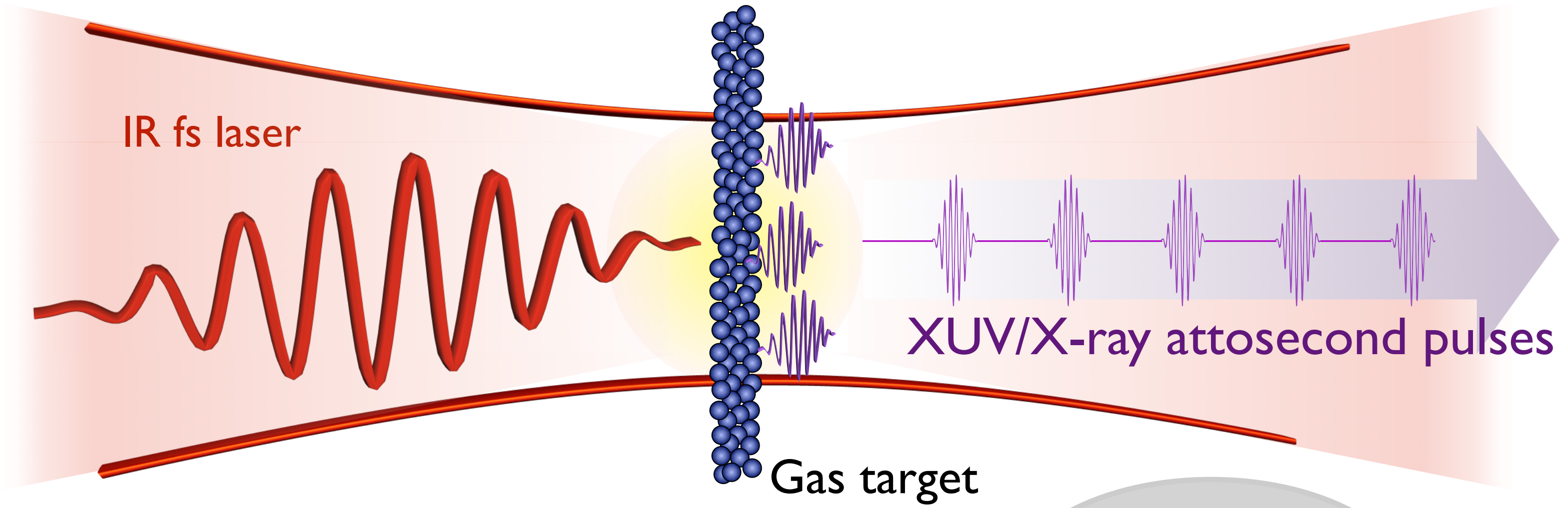

Perfect phase-matching $\Delta k_q = 0$

Phase-mismatch: $\Delta k_q = k_q - q k_1$

$$\Delta k_q \simeq \Delta k_q^{geom} + \Delta k_q^{\text{int}} + \Delta k_q^{f} + \Delta k_q^{b}$$

Optimal phase-matching: $\left|\Delta k_q^{f}\right| = \left|\Delta k_q^{b}\right| \rightarrow \Delta k_q = 0$

T. Popmintchev et al, PNAS 106, 10516 (2009)
Rundquist et al, Science 280 (1998)

Optimal phase-matching

$$\Delta k_q = k_q - q k_1 \simeq \Delta k_q^{geom} + \Delta k_q^{\text{int}} + \Delta k_q^{f} + \Delta k_q^{b}$$

$$\Delta k_q \simeq -\frac{4\pi^2}{\lambda_q}\left[\chi_f(\lambda_0) + \chi_b(\lambda_0)\right] \simeq q\left[\frac{P_f n_0 e^2 \lambda_0}{mc^2} - \frac{4\pi^2 (1 - P_f) n_0 \chi_b^0}{\lambda_0 \eta_0}\right]$$

$$\Delta k_q = 0 \rightarrow P_f^{opt} \approx \frac{\chi_b^0}{\eta_0}\left(\frac{e^2 \lambda_0}{4\pi mc^2} - \frac{\chi_b^0}{\eta_0}\right)^{-1}$$

Optimal ionized population,

$P_f^{opt} \rightarrow (\lambda_0, I)$

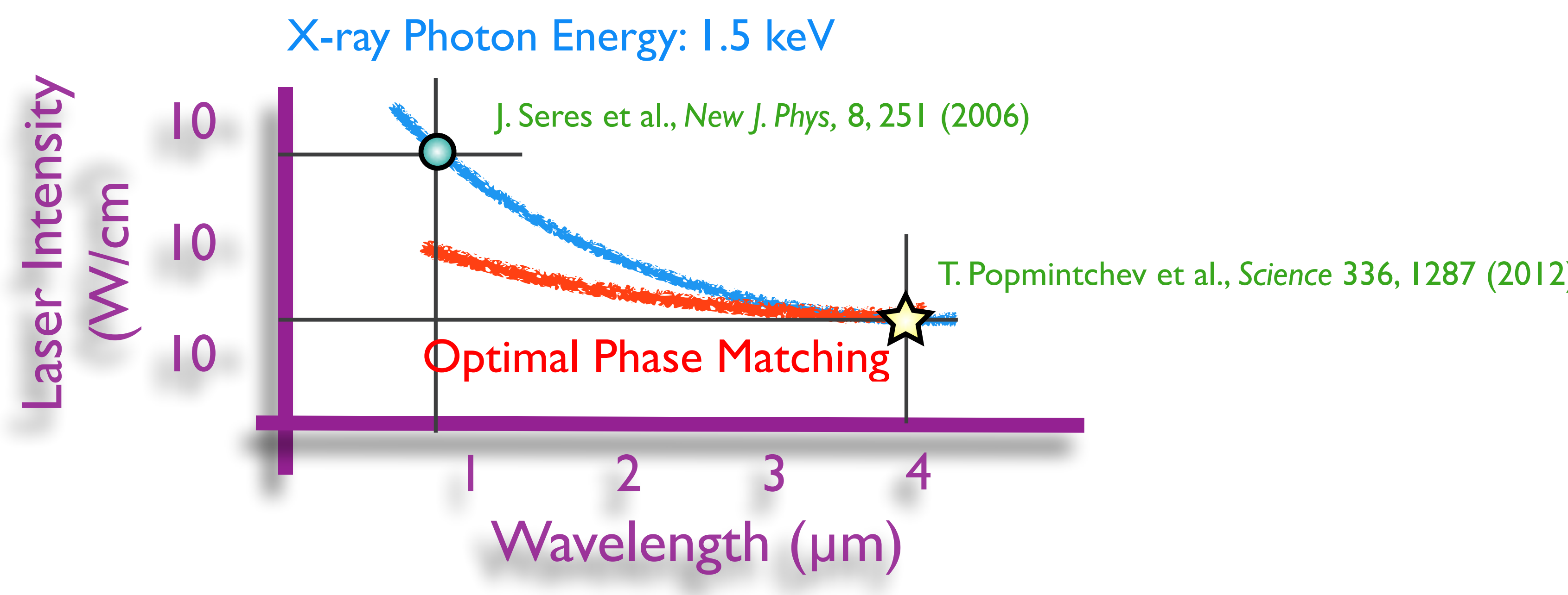

Time gated phase-matching

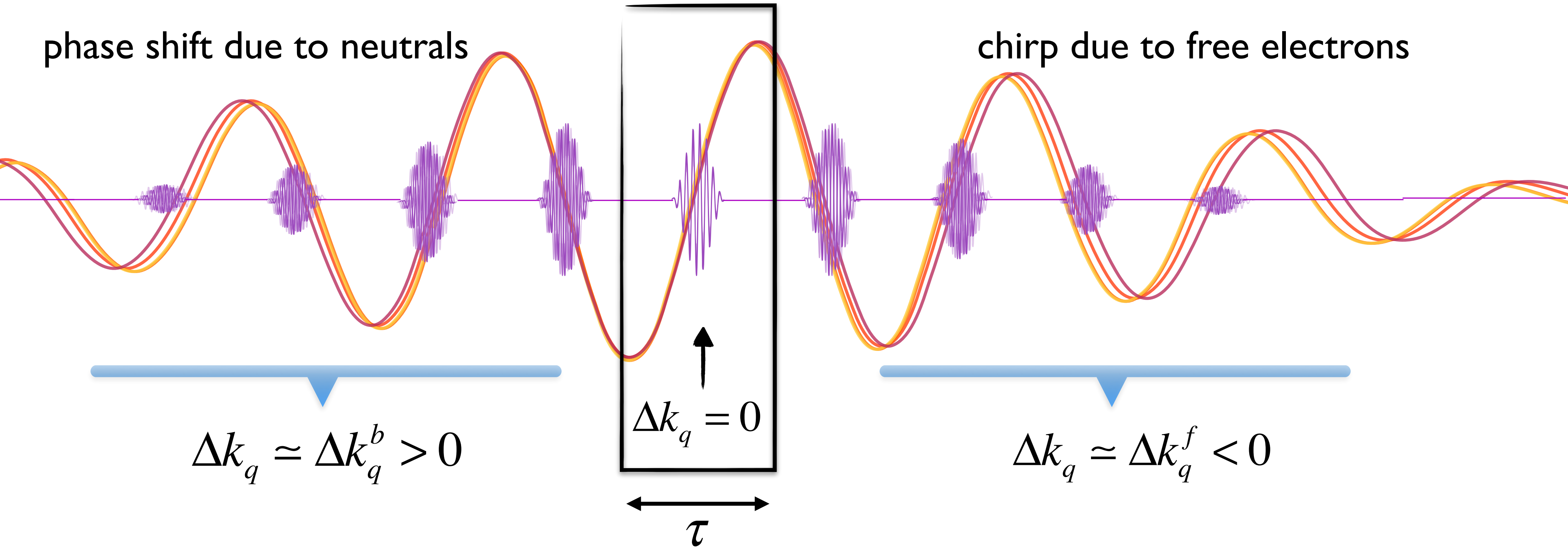

Size of the phase-matching window

$$\frac{1}{\tau} \propto \frac{\partial \Delta k_q}{\partial t} \propto {\lambda_0}^{1.5} P$$

3D simulations

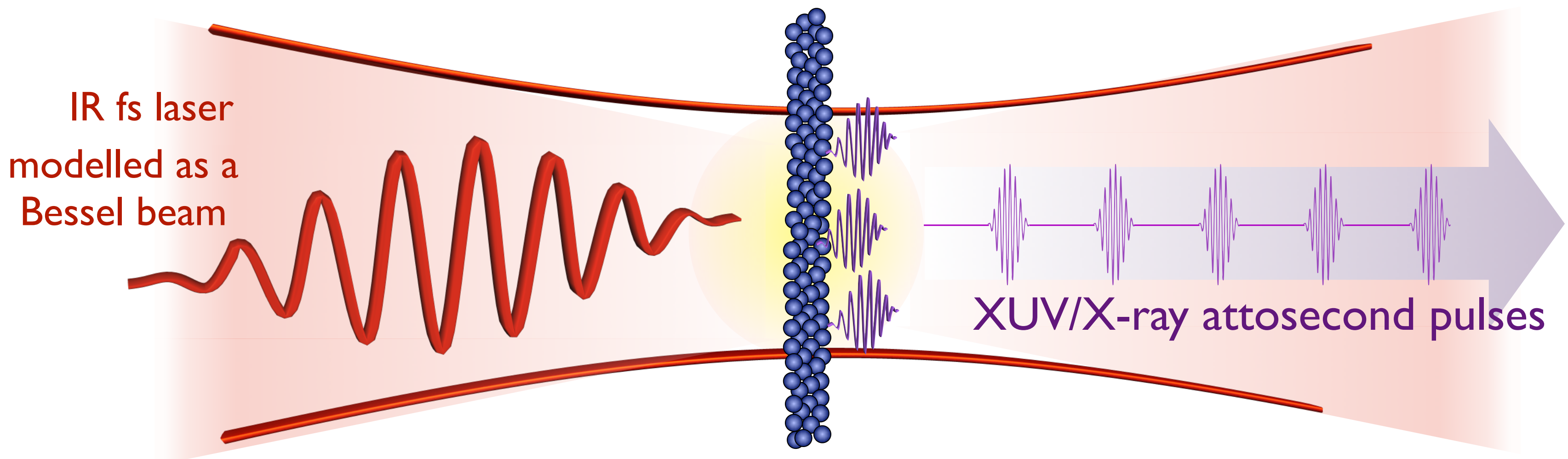

2 mm
Helium gas cell

0.8 μm
2.0 μm

Intensities given by phase-matching conditions

Theoretical Method:

- High-Harmonic Generation: SFA+
- Propagation: Discrete Dipole Approximation using Maxwell equations

C. Hernández-García, et al. Phys. Rev. A 82, 033432 (2010

3D simulations: 800 nm, 5.8 cycles

2 mm He gas cell, peak intensity $6.6\times10^{14}\,Wcm^{-2}$

$$\frac{\partial \Delta k_q}{\partial t} \propto \lambda_0^{\,1.5} P$$

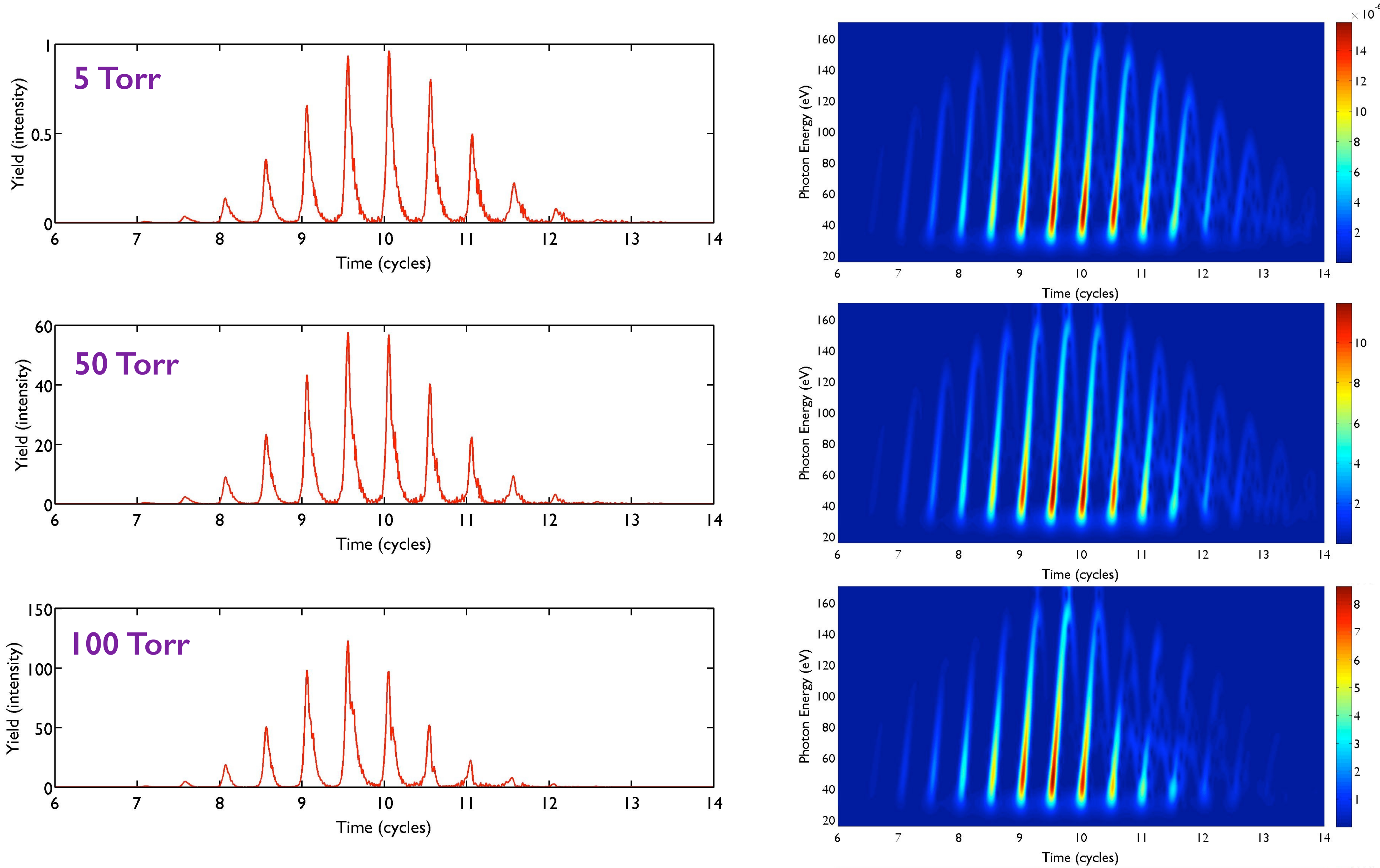

3D simulations: 2.0 μm, 5.8 cycles

2 mm He gas cell, peak intensity $4.4 \times 10^{14} Wcm^{-2}$

$$\frac{\partial \Delta k_q}{\partial t} \propto \lambda_0^{1.5} P$$

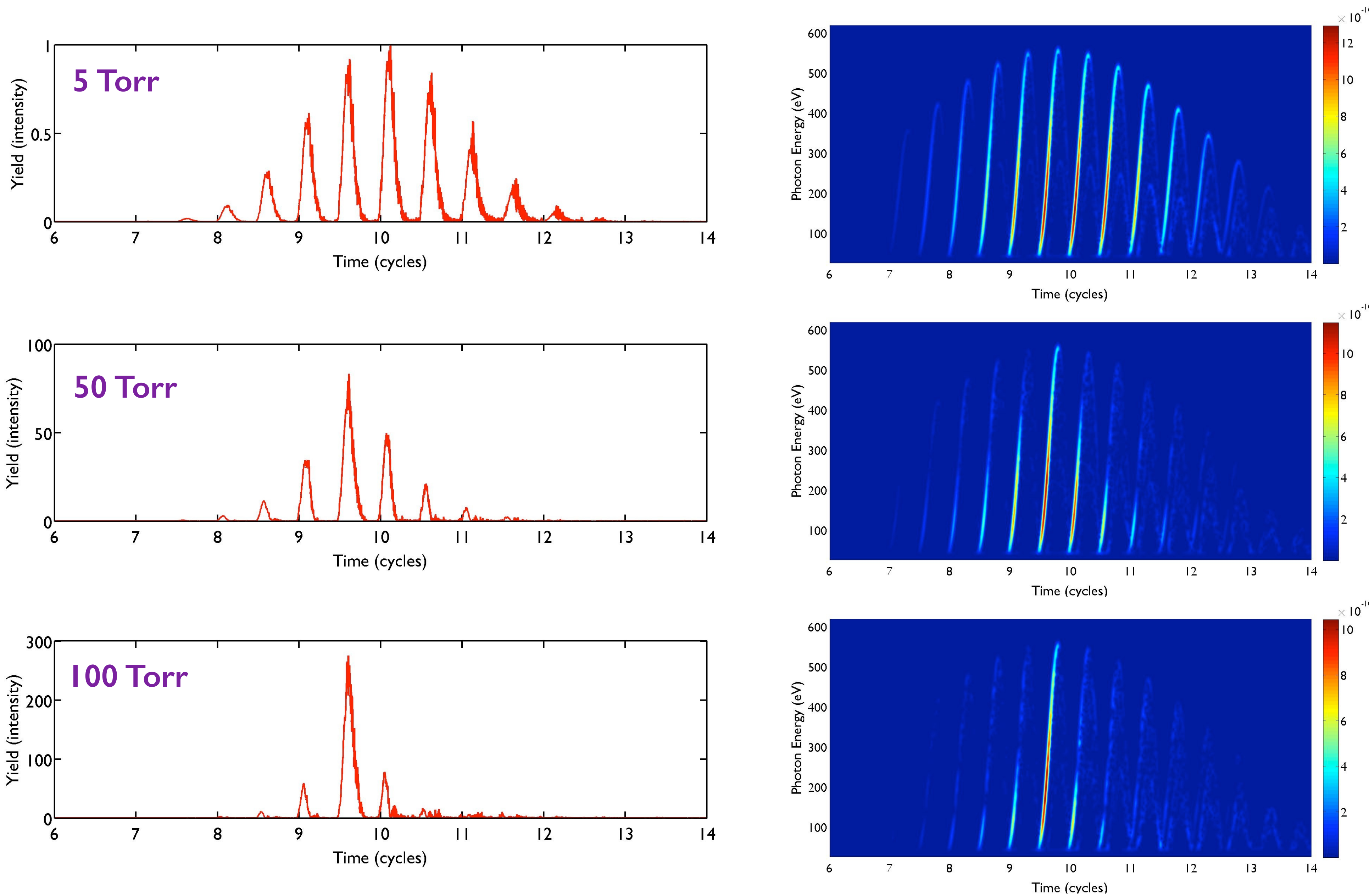

Phase-matching with multi-cycle pulses

2 mm He gas cell

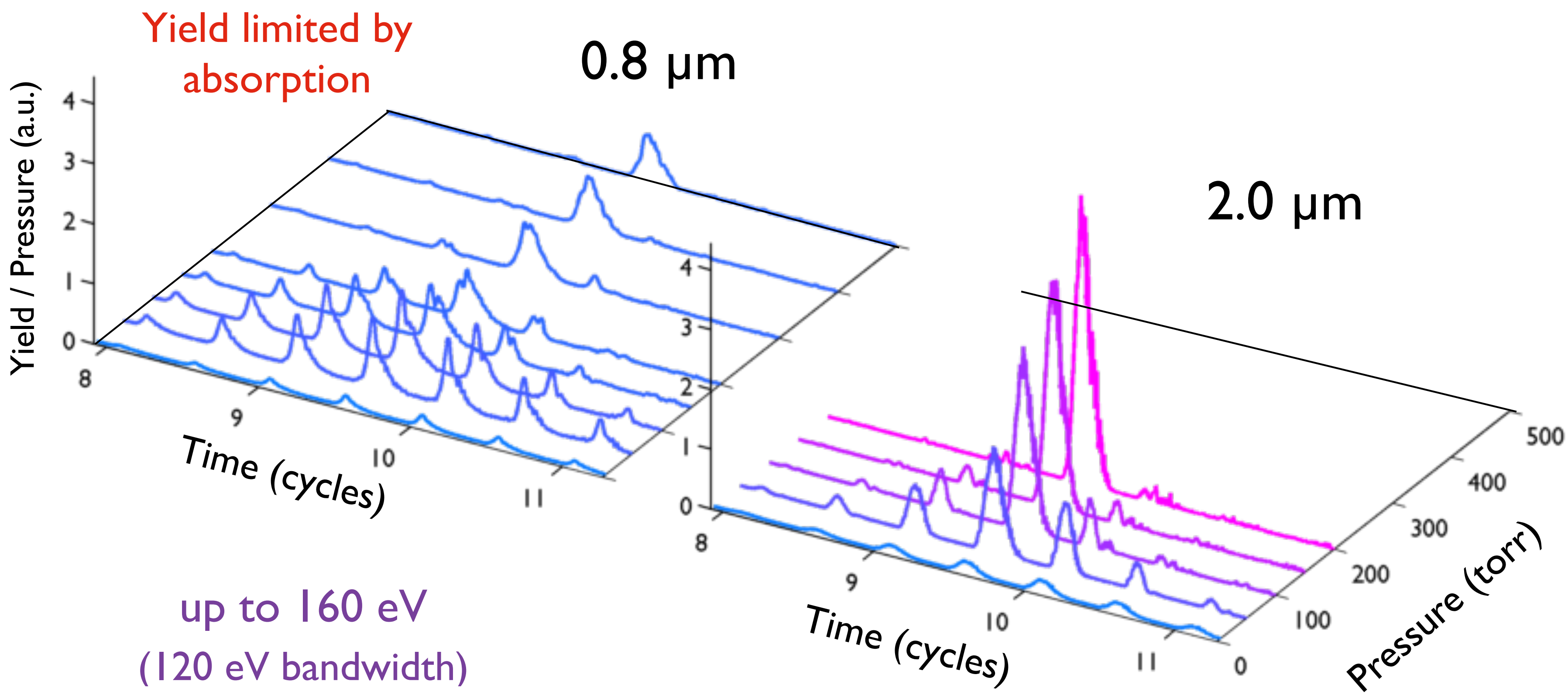

up to 160 eV
(120 eV bandwidth)

up to 550 eV
(500 eV bandwidth)

Experimental results

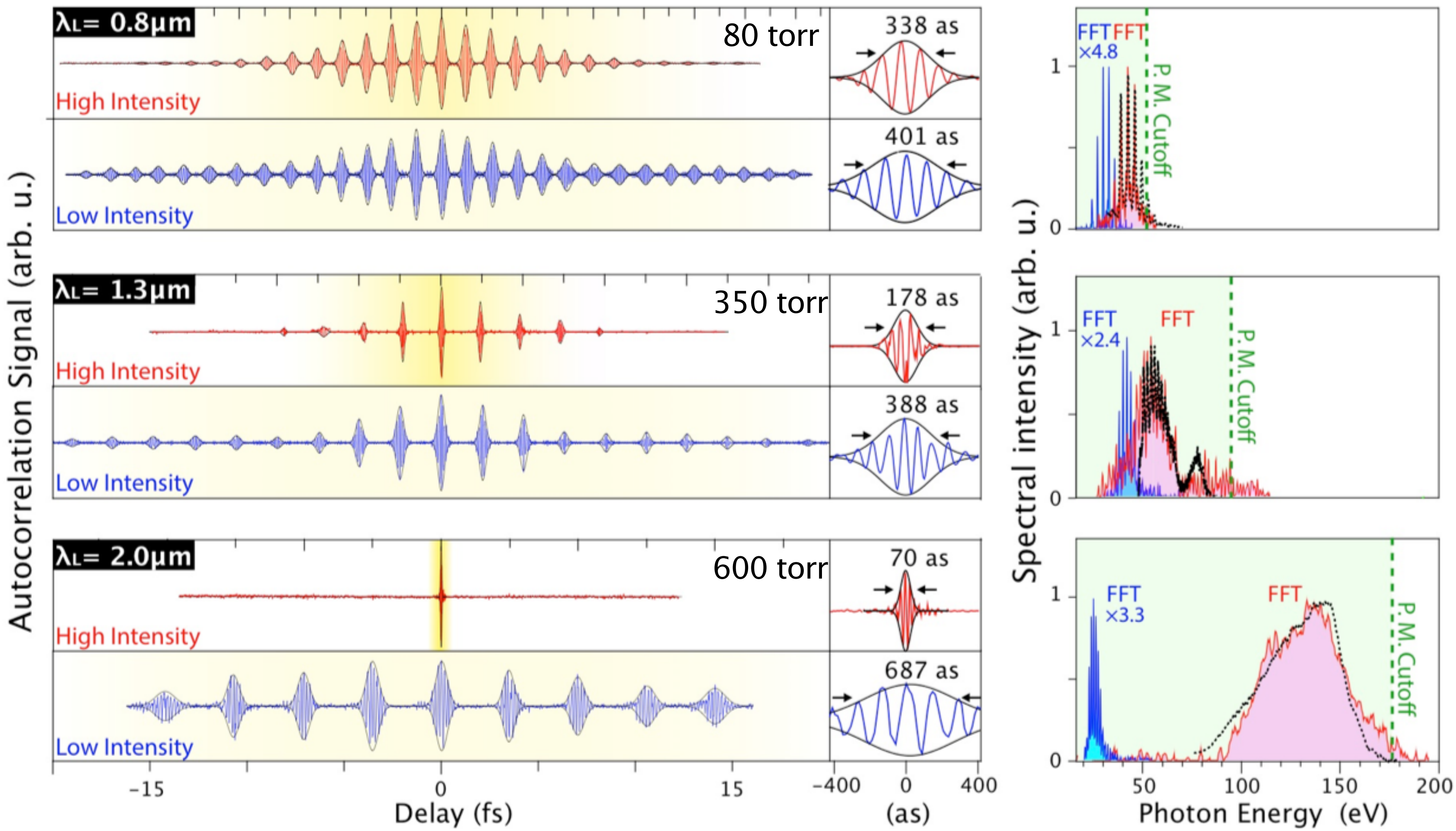

M.-C. Chen, C. Mancuso, C. Hernández-García, F. Dollar, B. Galloway, D. Popmintchev, B. Langdon, A. Auger, P.-C. Huang, B.C. Walker, L. Plaja, A. Jaron-Becker, A. Becker, M. M. Murnane, H. C. Kapteyn, T. Popmintchev, *PNAS* 111 (23), E2361-E2367 (2014)

Few-cycle vs Multi-cycle at 2 μm

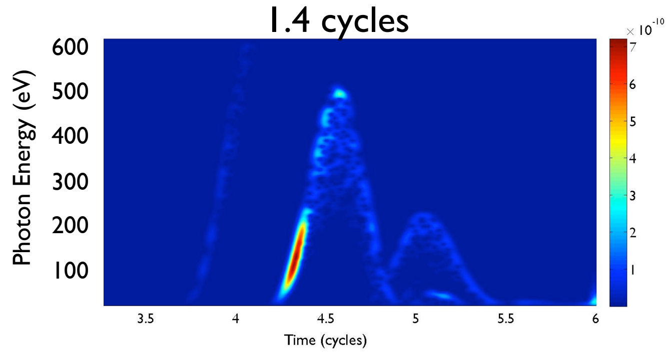

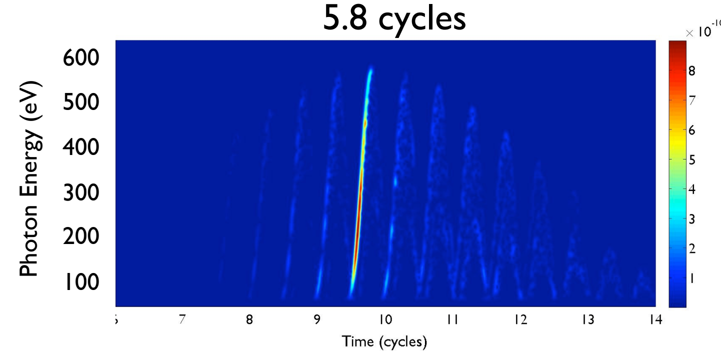

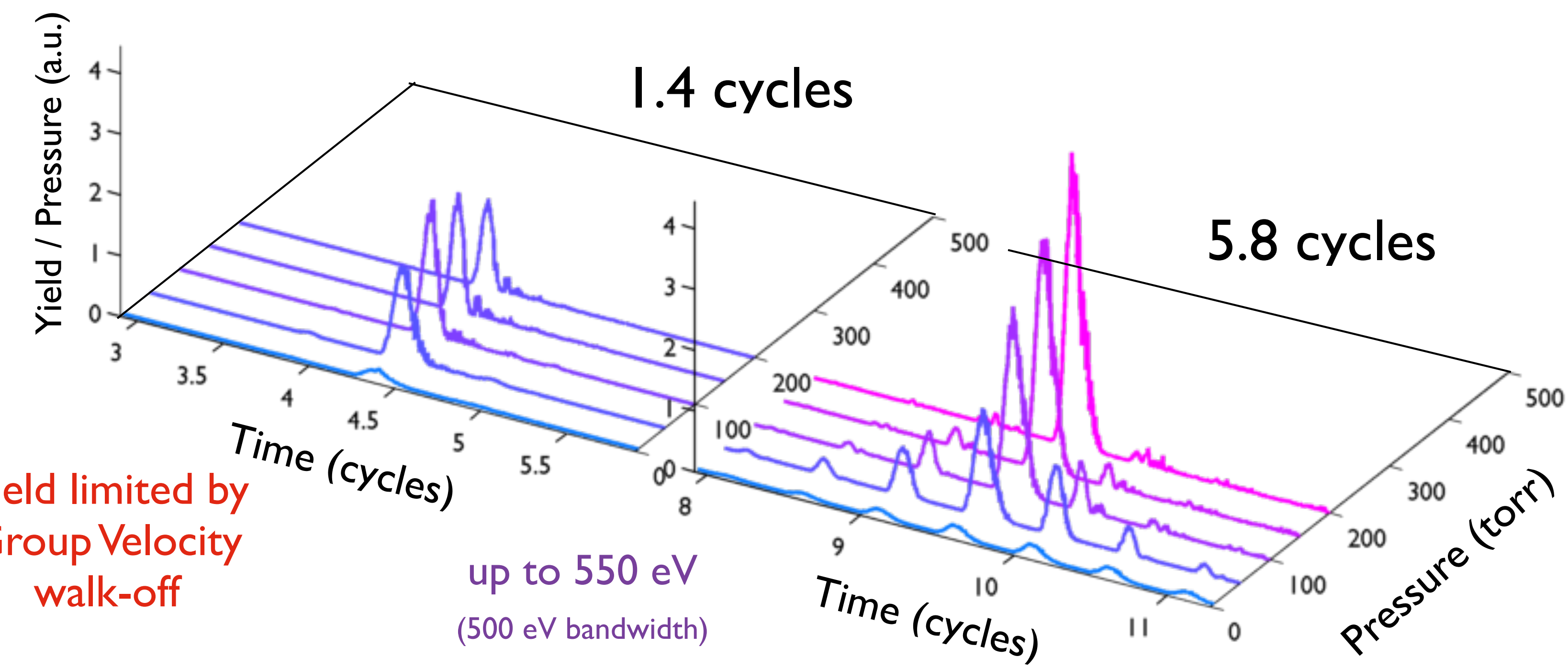

Yield limited by Group Velocity walk-off

up to 550 eV

(500 eV bandwidth)

Group velocity walk-off

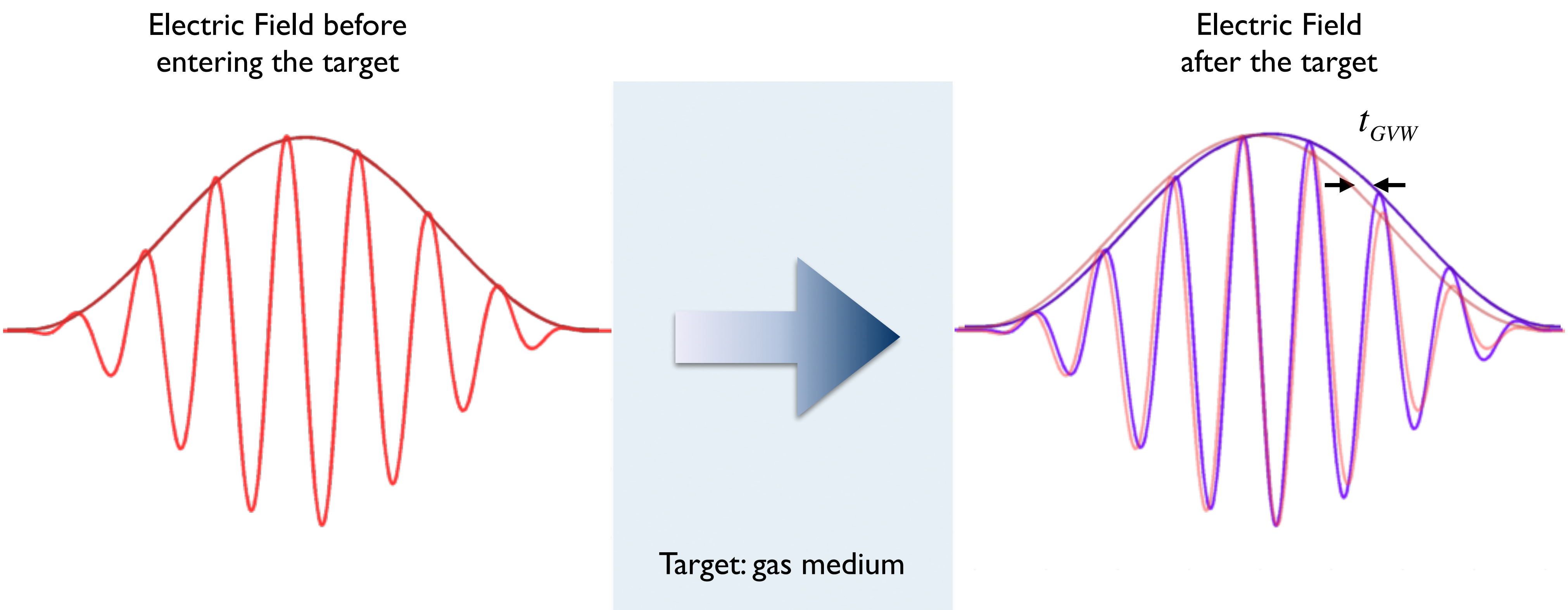

Group velocity: $$\frac{1}{v_g} - \frac{1}{v_{ph}} = \frac{\omega}{c}\frac{\partial n(\omega)}{\partial \omega}$$

Temporal delay due to group velocity walk-off $$t_{GVW} = \left(\frac{1}{v_g} - \frac{1}{c}\right) z$$

Group velocity matching:

Fundamental field travels with $v_g(\omega_0)$

Harmonic field travels with $v_g(q\omega_0) \approx c$

Effect of the group velocity walk-off on the carrier

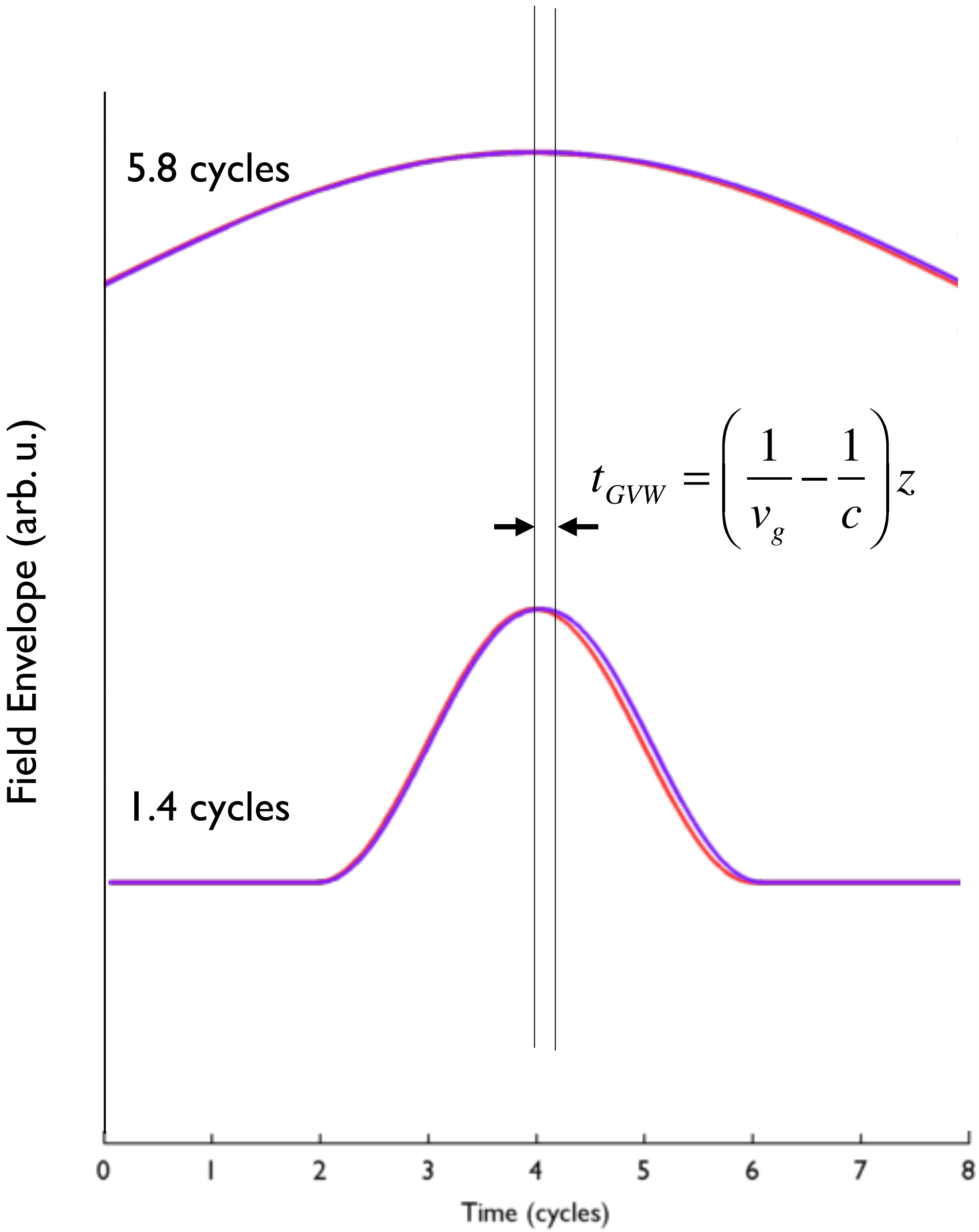

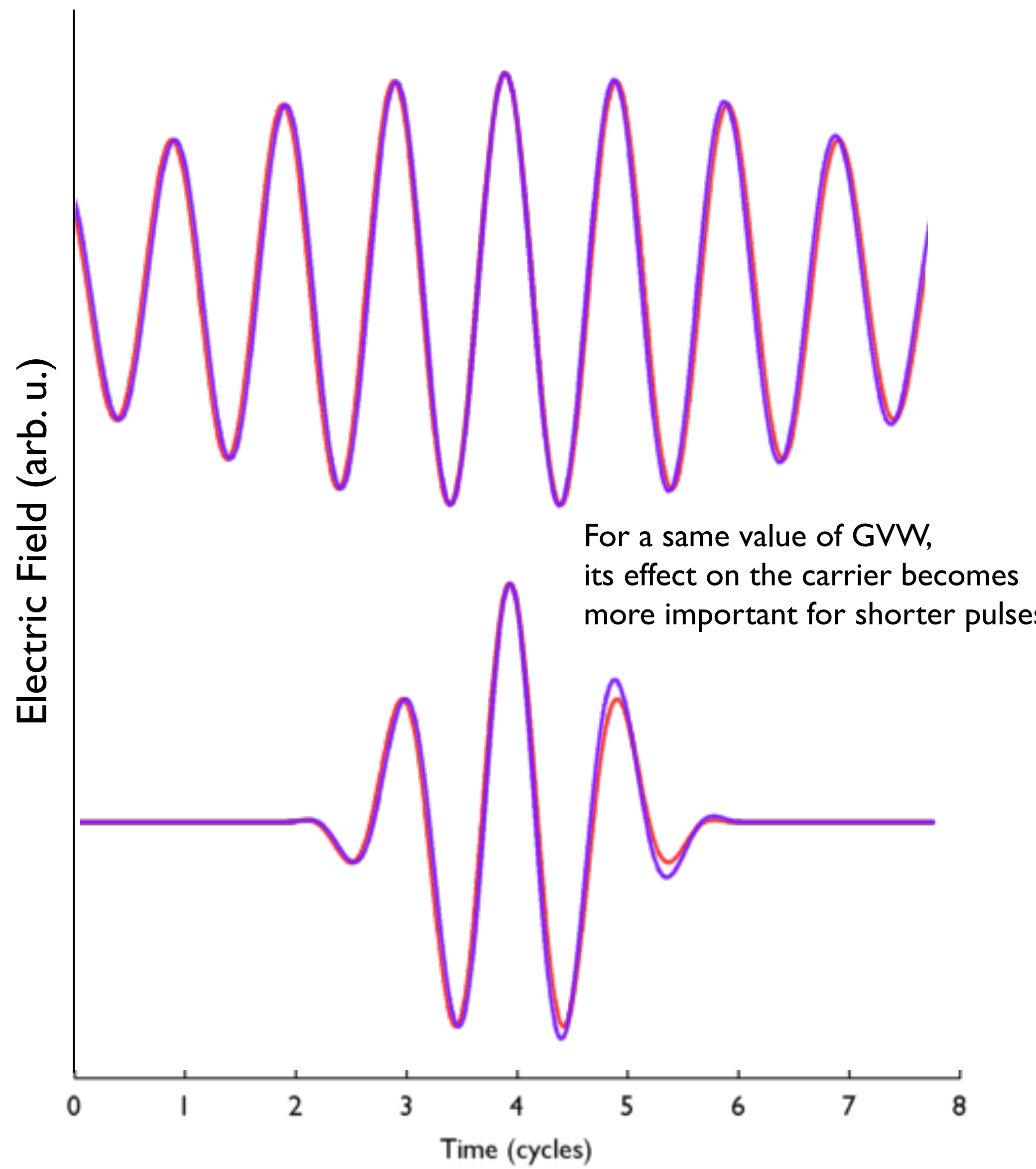

Isolated X-ray attosecond pulses

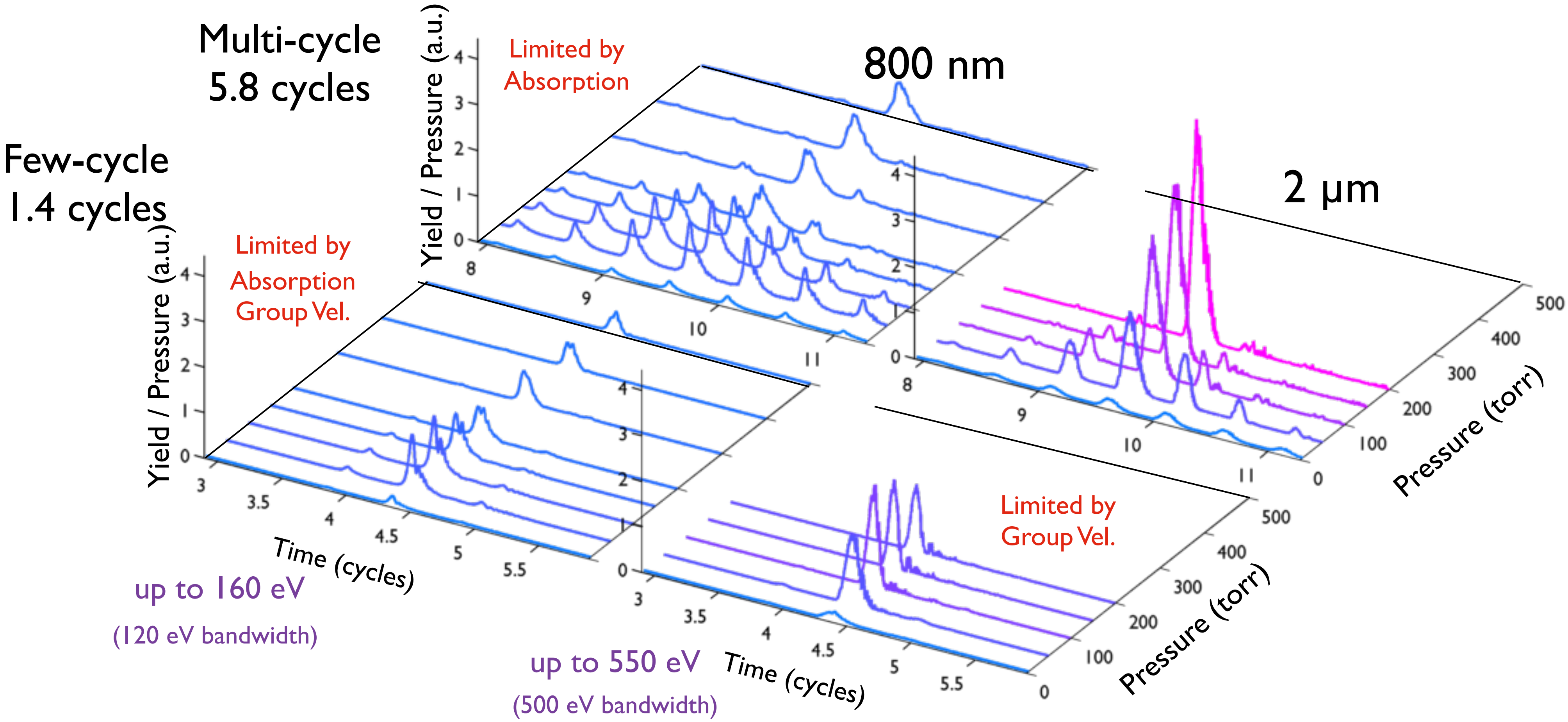

- We derive a route for **extending isolated attosecond pulses to the x-ray regime** by using mid-IR wavelengths.
- **Multi-cycle laser pulses** show better yield scaling due to group velocity walk-off.

Conclusions

- We propose a route for producing zeptosecond waveforms in the keV regime, driving HHG by mid-IR laser pulses.
- We demonstrate the generation of isolated attosecond pulses in the X-ray regime using mid-IR multi-cycle laser pulses.

carloshergar@jila.colorado.edu